Pontifícia Universidade Católica
do Rio de Janeiro

Isabela Cunha Maia Nobre

On the Protection of Fixed Service Receivers from the Interference Generated by Non-GSO Satellite Systems Operating in the 3.7-4.2 GHz Band

Dissertação de Mestrado

Dissertation presented to the Programa de Pós–graduação em Engenharia Elétrica of PUC-Rio in partial fulfilment of the requirements for the degree of Mestre em Engenharia Elétrica.

Advisor: Prof. José Mauro Pedro Fortes

Rio de Janeiro
July 2017

Pontifícia Universidade Católica
do Rio de Janeiro

Isabela Cunha Maia Nobre

On the Protection of Fixed Service Receivers from the Interference Generated by Non-GSO Satellite Systems Operating in the 3.7-4.2 GHz Band

Dissertation presented to the Programa de Pós–graduação em Engenharia Elétrica of PUC-Rio in partial fulfilment of the requirements for the degree of Mestre em Engenharia Elétrica. Approved by the undersigned Examination Committee.

Prof. José Mauro Pedro Fortes
Advisor
Centro de Estudos em Telecomunicações – PUC-Rio

Prof. Raimundo Sampaio Neto
Centro de Estudos em Telecomunicações – PUC-Rio

Prof. Pedro Henrique Gouvêa Coelho
Universidade do Estado do Rio de Janeiro – UERJ

Prof. Márcio da Silveira Carvalho
Vice Dean of Graduate Studies
Centro Técnico Científico – PUC-Rio

Rio de Janeiro, July 10th, 2017

Isabela Cunha Maia Nobre

Received the Bachelor of Science degree in Electrical Engineering from the Pontifícia Universidade Católica do Rio de Janeiro (Rio de Janeiro, Brazil) in 2015.

Bibliographic data

Cunha Maia Nobre, Isabela

On the Protection of Fixed Service Receivers from the Interference Generated by Non-GSO Satellite Systems Operating in the 3.7-4.2 GHz Band / Isabela Cunha Maia Nobre; advisor: José Mauro Pedro Fortes. – Rio de Janeiro: PUC-Rio, Centro de Estudos em Telecomunicações, 2017.

v., 70 f: il. color. ; 30 cm

Dissertação (mestrado) - Pontifícia Universidade Católica do Rio de Janeiro, Centro de Estudos em Telecomunicações.

Inclui bibliografia

1. Engenharia Elétrica – Tese. 2. Satélites não-geoestacionários. 3. Interferência. 4. Serviço Fixo Terrestre. 5. Teoria da Probabilidade. 6. Critérios de Proteção. 7. Densidade de Fluxo de Potência. I. Pedro Fortes, José Mauro. II. Pontifícia Universidade Católica do Rio de Janeiro. Centro de Estudos em Telecomunicações. III. Título.

CDD: 621.3

Acknowledgements

I would like to thank my advisor José Mauro, who agreed to work with me, for his advice, inspiration and friendship, whose wisdom and availability to always help me enabled the development of this work, teaching me so much in the process.

I would also like to give my special thanks to my parents whose unconditional love and unfailing support mean so much to me. In particular, I would also like to thank my father for lending me his computer to contribute to additional simulations needed.

I must express my gratitude to my friends who brought cheers to my life, giving me joy and energy to continue, and specially to my friend Julio, for all the many insightful discussions and help in theoretical problems.

I cannot forget to mention all of my family who gave me motivation and continuous encouragement in my pursuit. Special thanks to my grandmother Acilea who welcomed me in her home and my siblings Gabriela and Guilherme for their companionship and support.

I would like to acknowledge my fellow labmates at CETUC for their feedback, cooperation and friendship. Specifically Alberth and Americo for helping me with a few programming issues and for turning my computer on countless times so that I could remotely access it.

In addition, I am also grateful to PUC-Rio and CNPq for supporting this work.

Finally, I would like to thank God for His love, protection and spiritual guidance toward my dreams.

This accomplishment would not have been possible without you.
Thank you.

Abstract

Cunha Maia Nobre, Isabela; Pedro Fortes, José Mauro (Advisor). **On the Protection of Fixed Service Receivers from the Interference Generated by Non-GSO Satellite Systems Operating in the 3.7-4.2 GHz Band**. Rio de Janeiro, 2017. 70p. Dissertação de Mestrado – Centro de Estudos em Telecomunicações, Pontifícia Universidade Católica do Rio de Janeiro.

In this work, the current power-flux density limits in Article 21 of the ITU-R Radio Regulations for non-GSO systems operating in the 3.7-4.2 GHz band are analyzed. These limits aim the protection of Fixed Service receivers, operating in the same frequency band, from the interference produced by non-GSO satellite systems. The analysis was motivated by Resolution 157 [1] of the World Radiocommunication Conference 2015, that recognized the need for a revision of Article 21 with a view to enabling non-GSO systems to operate in these FSS frequency bands while ensuring that existing primary services are protected. In the analysis, five different *Walker Delta type* satellite constellation structures, adequately chosen, were considered. Results have shown that the current *pfd* limits may impose undue constraints to non-GSO systems operating in this band. Therefore, a methodology to investigate a more adequate *pfd* limiting mask is presented. The application of this methodology leads to an alternative mask that approaches the current *pfd* limits for the geostationary satellites when the number of satellites in the non-GSO interfering system is equal to one. An evaluation of the proposed *pfd* mask shows that it does not impose unnecessary constraints to the non-GSO satellite systems. This, along with other facts, indicates that the proposed *pfd* limits are, indeed, much more adequate than the current ones.

Keywords

Non-geostationary Satellites; Interference; Fixed Service ; Probability Theory; Protection Criteria; Power-flux Density.

Resumo

Cunha Maia Nobre, Isabela; Pedro Fortes, José Mauro. **Proteção de Receptores do Serviço Fixo Terrestre das Interferências Geradas por Sistemas Não-GEO Operando na Faixa de 3.7-4.2 GHz**. Rio de Janeiro, 2017. 70p. Dissertação de Mestrado – Centro de Estudos em Telecomunicações, Pontifícia Universidade Católica do Rio de Janeiro.

Neste trabalho, os limites atuais de densidade de fluxo de potência do Artigo 21 do Regulamento de Radiocomunicações da UIT para sistemas não-GEO operando na banda 3.7-4.2 GHz são analizados. Estes limtes visam proteger os receptores do Serviço Fixo Terrestre, operando na mesma faixa de frequência, das interferências produzidas por sistemas de satélites não geoestacionários. A análise foi motivada pela Resolução 157 [1] da Conferência Mundial de Radiocomunicações de 2015, que reconheceu a necessidade de uma revisão do Artigo 21 para que sistemas não-GEO possam operar nestas faixas de frequências assegurando, ao mesmo tempo, que os serviços primários existentes continuem protegidos. Na análise, cinco estruturas de constelações de satélites não-GEO do tipo *Walker Delta*, adequadamente escolhidas, foram consideradas. Resultados mostraram que os atuais limtes de *pfd* podem impor restrições indevidas aos sistemas não-GEO operando nesta faixa. Assim, uma metodologia para investigar uma máscara limitante de *pfd* mais adequada é apresentada. A aplicação desta metodologia leva a uma máscara alternativa que se aproxima dos limites atuais de *pfd* para satélites geoestacionários quando o número de satélites no sistema interferente não-GEO é igual a um. Uma avaliação da máscara de *pfd* proposta mostra que ela não impõe restrições desnecessárias aos sistemas de satélites não-GEO. Isto, junto a outros fatos, indica que os limites de *pfd* propostos são, de fato, muito mais adequados do que os atuais.

Palavras-chave

Satélites não-geoestacionários ; Interferência ; Serviço Fixo Terrestre ; Teoria da Probabilidade; Critérios de Proteção; Densidade de Fluxo de Potência

.

Table of contents

List of figures

Figure 2.1 Satellite interfering with a fixed service receiving antenna 17
Figure 2.1 Satellite interfering with a fixed service receiving antenna 17

Figure 2.2 Cumulative distribution of an interference that attends the protection criteria 22
Figure 2.2 Cumulative distribution of an interference that attends the protection criteria 22

Figure 2.3 values y_ℓ that satisfy $C_{\left(\frac{i_t}{N}\right)_{dB}}(y_\ell) = p_\ell$ 23
Figure 2.3 values y_ℓ that satisfy $C_{\left(\frac{i_t}{N}\right)_{dB}}(y_\ell) = p_\ell$ 23

Figure 2.4 Margins μ_ℓ 24
Figure 2.4 Margins μ_ℓ 24

Figure 3.1 Table 21-4 of Radio Regulations, Power flux-density limit 27
Figure 3.1 Table 21-4 of Radio Regulations, Power flux-density limit 27

Figure 3.2 Cumulative distribution of the total interfering power produced by 5 systems of type E into a FS receiver located at $\theta_{FS} = 40°$ and with antenna diameter of $D = 4.5$ meters, for 180 different values of azimuth α. 29
Figure 3.2 Cumulative distribution of the total interfering power produced by 5 systems of type E into a FS receiver located at $\theta_{FS} = 40°$ and with antenna diameter of $D = 4.5$ meters, for 180 different values of azimuth α. 29

Figure 3.3 Cumulative distribution of the total interfering power produced by 5 systems of type B into a FS receiver located at $\theta_{FS} = 20°$ and with antenna diameter of $D = 3.6$ meters, for 180 different values of azimuth α. 29
Figure 3.3 Cumulative distribution of the total interfering power produced by 5 systems of type B into a FS receiver located at $\theta_{FS} = 20°$ and with antenna diameter of $D = 3.6$ meters, for 180 different values of azimuth α. 29

Figure 4.2 Probability distribution function of the interference margin μ_ℓ for a FS receiver located at latitude ±10° and FS antenna diameter 3 meters. 42

Figure 4.3 Probability distribution function of the interference margin μ_ℓ for a FS receiver located at latitude ±20° and FS antenna diameter 3 meters. 43
Figure 4.3 Probability distribution function of the interference margin μ_ℓ for a FS receiver located at latitude ±20° and FS antenna diameter 3 meters. 43

Figure 4.4 Probability distribution function of the interference margin μ_ℓ for a FS receiver located at latitude ±30° and FS antenna diameter 3 meters. 44
Figure 4.4 Probability distribution function of the interference margin μ_ℓ for a FS receiver located at latitude ±30° and FS antenna diameter 3 meters. 44

Figure 4.5 Probability distribution function of the interference margin μ_ℓ for a FS receiver located at latitude ±40° and FS antenna diameter 3 meters. 45
Figure 4.5 Probability distribution function of the interference margin μ_ℓ for a FS receiver located at latitude ±40° and FS antenna diameter 3 meters. 45

Figure 4.6 Probability distribution function of the interference margin μ_ℓ for a FS receiver located at latitude 0° and FS antenna diameter 3.6 meters. 49
Figure 4.6 Probability distribution function of the interference margin μ_ℓ for a FS receiver located at latitude 0° and FS antenna diameter 3.6 meters. 49

Figure 4.7 Probability distribution function of the interference margin μ_ℓ for a FS receiver located at latitude ±10° and FS antenna diameter 3.6 meters. 50

Figure 4.13 Probability distribution function of the interference margin μ_ℓ for a FS receiver located at latitude ±20° and FS antenna diameter 4.5 meters. 58
Figure 4.13 Probability distribution function of the interference margin μ_ℓ for a FS receiver located at latitude ±20° and FS antenna diameter 4.5 meters. 58

Figure 4.14 Probability distribution function of the interference margin μ_ℓ for a FS receiver located at latitude ±30° and FS antenna diameter 4.5 meters. 59
Figure 4.14 Probability distribution function of the interference margin μ_ℓ for a FS receiver located at latitude ±30° and FS antenna diameter 4.5 meters. 59

Figure 4.15 Probability distribution function of the interference margin μ_ℓ for a FS receiver located at latitude ±40° and FS antenna diameter 4.5 meters. 60
Figure 4.15 Probability distribution function of the interference margin μ_ℓ for a FS receiver located at latitude ±40° and FS antenna diameter 4.5 meters. 60

Figure A.1 Problem geometry. 65
Figure A.1 Problem geometry. 65

Figure A.2 Base B and base B'. 66
Figure A.2 Base B and base B'. 66

Figure A.3 Azimuth and Elevation 67
Figure A.3 Azimuth and Elevation 67

List of tables

Imagination is more important than knowledge. For knowledge is limited to all we now know and understand, while imagination embraces the entire world, and all there ever will be to know and understand.

Albert Einstein.

1
Introduction

Satellite communication systems allow for information transmission between places on Earth, in a cheap and efficient way, regardless of their distances. The operation of such systems is accomplished in a complex way that requires planning and coordination, in an international level, so that all systems operating in the same frequency band are sufficiently protected from interferences generated by them. This coordination aims for the efficient use of orbital and spectral resources, which are limited, guaranteeing that they are equally accessible to all countries worldwide.

Before the 90's, the communication satellite systems mostly used geostationary satellites orbit (GSO). Until then, the Article 21 of the Radio Regulations of the International Telecommunications Unions (RR - ITU) [2] specified maximum limits for the power flux density produced on the Earth's surface by geostationary satellites in order to guarantee the protection of the terrestrial Fixed Services (FS) receivers. The protection of FS receivers against the interferences caused by non-GSO systems was not contemplated back then.

In 1997, with the objective of protecting the FS receivers from the interferences generated by the new non-GSO systems, the 1997 World Radiocommunication Conference - WRC'97 - [3] proposed studies for definition of additional power limits (e.g. the power-flux density pfd) that should be satisfied by non-GSO satellites to guarantee the protection of other FS systems. As a result, in the period of 1997-2000, investigations involving different kinds of non-GSO satellite constellations were carried out [4–8]. In all of them, the statistical behavior of the interferences generated by the non-GSO satellite systems was obtained via computer simulation of the satellites orbital movement. Based on these results, the WRC-2000 included, in Article 21 of the RR-ITU, maximum limits of pfd to be met by the non-GSO satellites [9]. However, such studies did not consider the highly elliptical orbit (HEO) satellite systems, a specific kind of non-GSO satellites with highly inclined orbit. Further studies were carried out [10–12] considering the applicability of Articles 21 of the Radio Regulations to HEO systems in different frequency bands. As a consequence, based on the results of these additional studies, the WRC-03 revised the Articles 21 again and defined new limits of pfd to be met by HEO systems [13] in

2003.

In view of the recent technological revolutions and the expansion of the frequency bands allocated to the Fixed Satellite Service for use by non-GSO non-geostationary satellite systems (non-GSO), the 2015 World Radiocommunication Conference (WRC-15) considered the benefits of expanding the frequency bands used by non-GSO systems. In particular, the 3700 - 4200 MHz bandwidth was added [1] which will improve the capacity and the spectral efficiency of the satellite communication systems. It was observed by the conference that the pfd limits indicated in Article 21 for this bandwidth were determined for the HEO orbits, but the limits of pfd to the non-GSO systems of different types of orbits still remain to be determined. The conference therefore recognized the need for a revision and confirmation of the current pfd values in Article 21, taking into account the characteristics of the new submitted systems. In this respect, the WRC-15 has approved Resolution 157 [1] which points out to the necessity of studies that handle the technical and operational challenges involving non-geostationary systems operating in these new frequency bands.

There is currently a proposition, in light of the arguments presented here, within the ITU to investigate the non-GSO system in the 3700 - 4200 MHz bandwidth for the revision of Article 21. The results of these studies should allow the operation of new systems, while ensuring the fulfillment of the protection criteria previously defined for the FS.

The objective of the study presented in this MSc Thesis is to develop an analysis aiming to provide technical support for the revision of Article 21 of the RR-ITU by the upcoming 2019 World Radiocommunication Conference (WRC-19).

2
Problem Description and Mathematical Modeling

In this chapter, the mathematical and theoretical basis used to model the interference produced by non-GSO satellite systems on fixed service receivers operating in the same frequency band is described. In addition, the FS protection criterion considered in the interference assessment is presented and the concept of interference margin is defined.

2.1
Problem Description

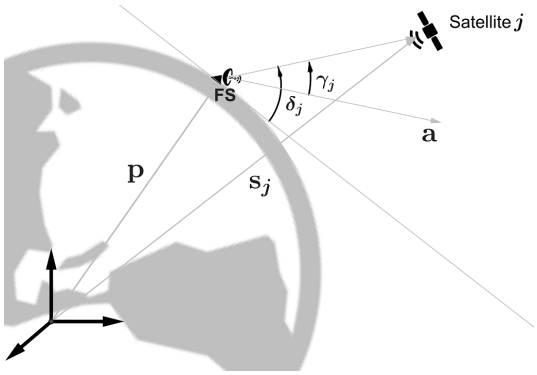

Figure 2.1: Satellite interfering with a fixed service receiving antenna

Consider Figure 2.1, where a satellite of a non-GSO system interferes with a fixed service receiver operating in the same frequency band. As observed, only one satellite (Satellite j), located at position $\mathbf{s}_j$, is shown. The FS victim receiver is located at position $\mathbf{p}$ and has a receiving antenna pointing at the direction of vector $\mathbf{a}$. The angles δ_j and γ_j represent, respectively, the interfering signal arrival angle and the FS receiving antenna off-axis angle in the direction of the interfering satellite.

If $\delta_j > 0$ (the satellite is visible by the earth station), then the interfering power reaching the FS receiver is given by

$$i(\gamma_j, \delta_j) = \frac{G(\gamma_j)\lambda^2}{4\pi L_{FS}}\, pfd(\delta_j). \tag{2-1}$$

Otherwise (satellite not visible), the interference is zero. In (2-1), $G(\gamma_j)$ is the FS earth station antenna gain in the direction of Satellite j, λ is the wavelength

corresponding to the signal's central frequency, L_{FS} is FS antenna feeder loss and pfd is the power flux-density delivered by the satellite on the Earth's surface at the FS location, which depends on the arrival angle δ_j.

The angle γ_j depends only on the vectors $\mathbf{p}$, $\mathbf{s}_j$ and $\mathbf{a}$, and the angle δ_j depends only on $\mathbf{p}$ and $\mathbf{s}_j$ (details in the Appendix). Thus, (2-1) can be rewritten as

$$i(\mathbf{p}, \mathbf{s}_j, \mathbf{a}) = \frac{G(\mathbf{p}, \mathbf{s}_j, \mathbf{a})\lambda^2}{4\pi L_{FS}} \, pfd(\mathbf{p}, \mathbf{s}_j). \tag{2-2}$$

The direction of the vector $\mathbf{a}$ depends on the azimuth α and on the elevation ϵ of the earth station antenna (see the Appendix). Both are defined in local coordinates, on a basis centered at the location. This means that (2-2) can be alternatively written as

$$i(\mathbf{p}, \mathbf{s}_j, \alpha, \epsilon) = \frac{G(\mathbf{p}, \mathbf{s}_j, \alpha, \epsilon)\lambda^2}{4\pi L_{FS}} \, pfd(\mathbf{p}, \mathbf{s}_j). \tag{2-3}$$

Note that for fixed values of the FS position $\mathbf{p}$ and the elevation ϵ of the FS receiving antenna, the interfering power in (2-3) will depend on $\mathbf{s}_j$ and α, that is,

$$i(\mathbf{s}_j, \alpha) = \frac{G(\mathbf{s}_j, \alpha)\lambda^2}{4\pi L_{FS}} \, pfd(\mathbf{s}_j). \tag{2-4}$$

The satellite position $\mathbf{s}_j$ is usually given in spherical coordinates, in terms of its latitude θ_j, longitude ϕ_j and height r_j:

$$\mathbf{s}_j = \begin{pmatrix} \theta_j \\ \phi_j \\ r_j \end{pmatrix}. \tag{2-5}$$

The aggregate interference due to all satellites in the non-GSO constellation is given by

$$i_{agg}(\mathbf{s}, \alpha) = \sum_{j=0}^{N-1} i(\mathbf{s}_j, \alpha), \tag{2-6}$$

where $\mathbf{s}$ is the 3N-dimensional vector containing the positions of all non-GSO satellites, that is,

$$\mathbf{s} = \begin{pmatrix} \mathbf{s}_0 \\ \mathbf{s}_1 \\ \vdots \\ \mathbf{s}_N \end{pmatrix}, \tag{2-7}$$

and $i(\mathbf{s}_j, \alpha)$ is given by (2-4).

2.2 Cumulative Distribution Function

In this work, the non-GSO satellite positions $\{\mathbf{s}_j, j = 0, \ldots, N-1\}$ and the azimuth α of the FS receiving antenna are modeled as random variables. As a consequence, the aggregate interfering power i_{agg} is also a random variable. Also, due to the circular *Walker Delta* structure [14] assumed for the non-

GSO satellite constellation, the positions of the satellites in the non-GSO system are not independent. Indeed, if the position of one of the satellites (here called a reference satellite) is known, the positions of all other satellites can be determined. Let then $\mathbf{s}_0$ be the position of the reference satellite. We then have

$$\mathbf{s}_j = \mathbf{F}_j(\mathbf{s}_0) \quad , \quad j = 1, \ldots, N-1 \tag{2-8}$$

with the functions $\{\mathbf{F}_j(\cdot), j = 1, \ldots, N-1\}$ defined by the *Walker Delta* constelation structure.

Thus, (2-6) becomes

$$i_{agg}(\mathbf{s}_0, \alpha) = \sum_{j=0}^{N-1} i(\mathbf{F}_j(\mathbf{s}_0), \alpha), \tag{2-9}$$

meaning that the aggregate interfering power is indeed a function of two statistically independent random variables, $\mathbf{s}_0$ and α.

The cumulative distribution function of the random variable i_{agg} is given by

$$C_{i_{agg}}(I) = P(i_{agg} > I) = \int_I^\infty p_{i_{agg}}(v)\, dv, \tag{2-10}$$

where $p_{i_{agg}}(I)$ is the probability density function of i_{agg}. Noting that $p_{i_{agg}}(I)$ can be expressed as (Ω_α and $\Omega_{\mathbf{S}}$ are the domains of A and $\mathbf{S}$, respectively)

$$p_{i_{agg}}(I) = \int_{\Omega_\alpha} \int_{\Omega_{\mathbf{S}}} p_{i_{agg},\alpha,\mathbf{s}_0}(I, A, \mathbf{S})\, dA\, d\mathbf{S}, \tag{2-11}$$

and that

$$p_{i_{agg},\alpha,\mathbf{s}_0}(I, A, \mathbf{S}) = p_{i_{agg},\mathbf{s}_0|\alpha=A}(I, \mathbf{S})\, p_\alpha(A), \tag{2-12}$$

it is possible to rewrite the cumulative distribution function in (2-10) as

$$C_{i_{agg}}(I) = \int_I^\infty \int_{\Omega_\alpha} \int_{\Omega_{\mathbf{S}}} p_{i_{agg},\mathbf{s}_0|\alpha=A}(v, \mathbf{S})\, p_\alpha(A)\, dA\, d\mathbf{S}\, dv \tag{2-13}$$

or

$$C_{i_{agg}}(I) = \int_{\Omega_\alpha} p_\alpha(A)\, C_{i_{agg}|\alpha=A}(I)\, dA, \tag{2-14}$$

with

$$C_{i_{agg}|\alpha=A}(I) = P(i_{agg} > I|\alpha = A) = \int_I^\infty \int_{\Omega_{\mathbf{S}}} p_{i_{agg},\mathbf{s}_0|\alpha=A}(v, \mathbf{S})\, d\mathbf{S}\, dv. \tag{2-15}$$

The inner integral in (2-15) can be written as

$$\int_{\Omega_{\mathbf{S}}} p_{i_{agg},\mathbf{s}_0|\alpha=A}(v, \mathbf{S})\, d\mathbf{S} = \int_{\Omega_{\mathbf{S}}} p_{i_{agg}|\mathbf{s}_0=\mathbf{S},\alpha=A}(v)\, p_{\mathbf{s}_0|\alpha=A}(\mathbf{S})\, d\mathbf{S}, \tag{2-16}$$

which, assuming that the random variables $\mathbf{s}_0$ and α are statistically independent, becomes

$$\int_{\Omega_{\mathbf{S}}} p_{i_{agg},\mathbf{s}_0|\alpha=A}(v, \mathbf{S})\, d\mathbf{S} = \int_{\Omega_{\mathbf{S}}} p_{i_{agg}|\mathbf{s}_0=\mathbf{S},\alpha=A}(v)\, p_{\mathbf{s}_0}(\mathbf{S})\, d\mathbf{S}. \tag{2-17}$$

From (2-15) and (2-17) we have

$$C_{i_{agg}|\alpha=A}(I) = P(i_{agg} > I|\alpha = A) = \int_I^\infty \int_{\Omega_{\mathbf{S}}} p_{i_{agg}|\mathbf{s}_0=\mathbf{S},\alpha=A}(v)\; p_{\mathbf{s}_0}(\mathbf{S})\; d\mathbf{S}\; dv, \tag{2-18}$$

or

$$C_{i_{agg}|\alpha=A}(I) = \int_I^\infty p_{i_{agg}|\alpha=A}(v)\; dv, \tag{2-19}$$

with

$$p_{i_{agg}|\alpha=A}(I) = \int_{\Omega_{\mathbf{S}}} p_{i_{agg}|\mathbf{s}_0=\mathbf{S},\alpha=A}(I)\; p_{\mathbf{s}_0}(\mathbf{S})\; d\mathbf{S}. \tag{2-20}$$

Note that, given $\mathbf{s}_0 = \mathbf{S}$ and $\alpha = A$, i_{agg} assumes a constant value, say $\mathcal{I}_{agg}(\mathbf{S}, A)$, with probability 1, hence,

$$p_{i_{agg}|\mathbf{s}_0=\mathbf{S},\alpha=A}(I) = \delta(I - \mathcal{I}_{agg}(\mathbf{S}, A)), \tag{2-21}$$

where $\delta(\cdot)$ is the Dirac delta function. As a consequence, (2-18) and (2-20) become, respectively,

$$C_{i_{agg}|\alpha=A}(I) = \int_{\Omega_{\mathbf{S}}} \int_I^\infty \delta(v - \mathcal{I}_{agg}(\mathbf{S}, A))\; dv\; p_{\mathbf{s}_0}(\mathbf{S})\; d\mathbf{S}, \tag{2-22}$$

and

$$p_{i_{agg}|\alpha=A}(I) = \int_{\Omega_{\mathbf{S}}} \delta(I - \mathcal{I}_{agg}(\mathbf{S}, A))\; p_{\mathbf{s}_0}(\mathbf{S})\; d\mathbf{S}. \tag{2-23}$$

Also, (2-22) can be further simplified to

$$C_{i_{agg}|\alpha=A}(I) = \int_{\Omega_{\mathbf{S}}} u(\mathcal{I}_{agg}(\mathbf{S}, A) - I)\; p_{\mathbf{s}_0}(\mathbf{S})\; d\mathbf{S}, \tag{2-24}$$

where $u(\cdot)$ is the unitary step function.

The integral in (2-24) can be determined either by using the Monte Carlo Method (simulation) or by using the Analytical Method presented in [15]. In this work we have chosen to use the Analytical Method since it provides a very good accuracy in the very low probability ranges of $C_{i_{agg}|\alpha=A}(I)$. Such accuracy with the Monte Carlo Method could require a prohibitive amount of computer time.

2.3 Multiple Systems

The result in (2-24) (also in (2-23)) provides the statistical behavior of the interfering power produced by the satellites of a single non-GSO satellite system into an FS receiver located at a fixed geographical position and with its receiving antenna pointing at a specific direction. The receiving antenna pointing direction is characterized by a fixed known elevation and a given azimuth $\alpha = A$.

When multiple non-GSO satellite systems are considered, the FS receiver

experiences the aggregate interference due to all non-GSO systems operating simultaneously in the same frequency band. Let then i_t be the total interfering power produced by K non-GSO systems into the FS receiver and let $\{i_{agg_k}, k = 1, 2, ..., K\}$ be the interfering power due to the kth non-GSO system. We then have

$$i_t = \sum_{k=1}^{K} i_{agg_k} \tag{2-25}$$

where

$$i_{agg_k} = i_{agg}(\mathbf{s}_{0_k}, \alpha) \tag{2-26}$$

with $i_{agg}(\mathbf{s}_{0_k}, \alpha)$ given by(2-9) and $\mathbf{s}_{0_k}$ denoting the position of the reference satellite in the k-th non-GSO system.

It is assumed that the positions $\{\mathbf{s}_{0_1}, \mathbf{s}_{0_2}, \ldots, \mathbf{s}_{0_K}\}$ of the reference satellites in the K interfering non-GSO systems are statistically independent. As a consequence, given $\alpha = A$, the random variables $\{i_{agg_k}, k = 1, 2...K\}$ are also statistically independent. The conditional probability density function of the total interference power i_t, given $\alpha = A$, can then be written as [16].

$$p_{i_t|\alpha=A}(I) = p_{i_{agg1}|\alpha=A}(I) * p_{i_{agg2}|\alpha=A}(I) * ... * p_{i_{aggK}|\alpha=A}(I). \tag{2-27}$$

The conditional cumulative distribution function of i_t, given $\alpha = A$, can be obtained by integrating (2-27), that is,

$$C_{i_t|\alpha=A}(I) = P(i_t > I|\alpha = A) = \int_I^{\infty} p_{i_t|\alpha=A}(u)\, du. \tag{2-28}$$

Finally, the conditional cumulative distribution function of the interference to noise ratio $i_t/\mathcal{N}$ (with $\mathcal{N}$ denoting the victim receiver thermal noise power) is given by

$$C_{\frac{i_t}{\mathcal{N}}|\alpha=A}(\eta) = P\left(\frac{i_t}{\mathcal{N}} > \eta|\alpha = A\right) = C_{i_t|\alpha=A}(\mathcal{N}\eta), \tag{2-29}$$

and if $\frac{i_t}{\mathcal{N}}$ is given in dB, we have

$$C_{\left(\frac{i_t}{\mathcal{N}}\right)_{dB}|\alpha=A}(\eta) = C_{\frac{i_t}{\mathcal{N}}|\alpha=A}(10^{\frac{\eta}{10}}) = C_{i_t|\alpha=A}(\mathcal{N}10^{\frac{\eta}{10}}). \tag{2-30}$$

2.4 Protection Criteria

The Recommendation ITU-R F.1495 [17] defines interference criteria to protect the Fixed Service from time varying aggregate interference from other radiocommunication services in the 17.7-19.3 GHz band. Currently, there is no equivalent protection criteria for the 4GHz band and we believe that, if criteria are developed for the 4 GHz band, they would not be much different from those in Recommendation ITU-R F.1495. For this reason, in the absence of specific criteria for the 4GHz band, the criteria in Recommendation ITU-R

F.1495 will be considered here. Specifically, the Recommendation states that,

- for the long-term,
  - the value of $(i_t/\mathcal{N})_{dB} = -10dB$ should not be exceeded for more than 20% of the time;
- for the short-term,
  - the value of $(i_t/\mathcal{N})_{dB} = 14dB$ should not be exceeded for more than 0.01% of the time; and
  - the value of $(i_t/\mathcal{N})_{dB} = 18dB$ should not be exceeded for more than 0.0003% of the time.

Note that, in terms of probability, these criteria can be expressed as

$$P\Big((i_t/\mathcal{N})_{dB} > L_\ell\Big) \leq p_\ell, \quad \ell = 1, 2, 3, \tag{2-31}$$

or,

$$C_{(\frac{i_t}{\mathcal{N}})_{dB}}(L_\ell) \leq p_\ell, \quad \ell = 1, 2, 3, \tag{2-32}$$

with $L_1 = -10$dB, $L_2 = 14$dB and $L_3 = 18$dB and with $p_1 = 0.2$ (long-term), $p_2 = 0.0001$ (first short-term) and $p_3 = 0.000003$ (second short-term). As illustrated in Figure 2.2, these criteria require that the cumulative distribution function of the interference to noise ratio (expressed in dB) passes below the shown asterisks.

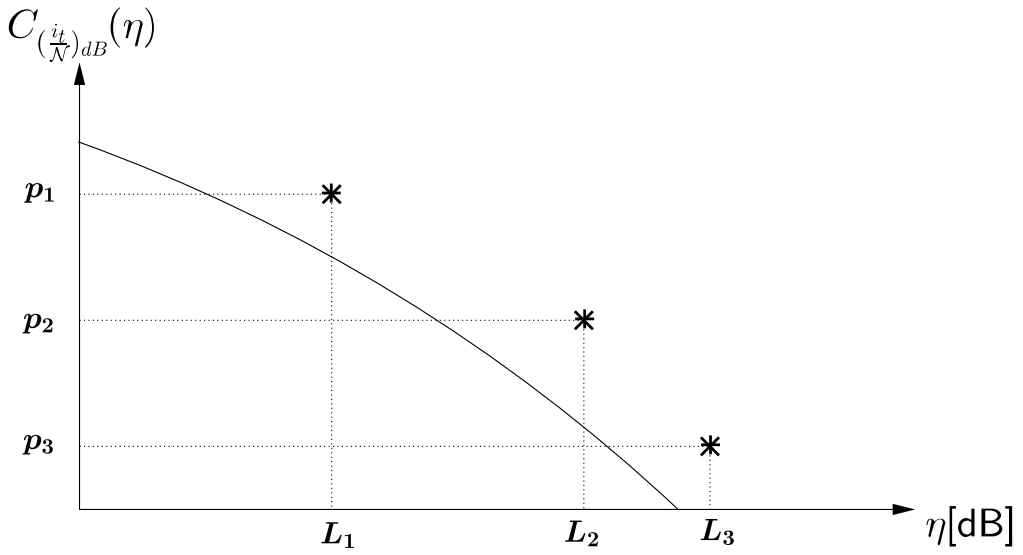

Figure 2.2: Cumulative distribution of an interference that attends the protection criteria

2.5 Interference Margins

Let $\{y_\ell,\ \ell = 1, 2, 3\}$ be the interference to noise ratio level exceeded with probability p_ℓ, that is, the values y_ℓ that satisfy the condition

$$C_{\left(\frac{i_t}{N}\right)_{dB}}(y_\ell) = p_\ell, \quad \ell = 1, 2, 3. \tag{2-33}$$

These values are illustrated in Figure 2.3.

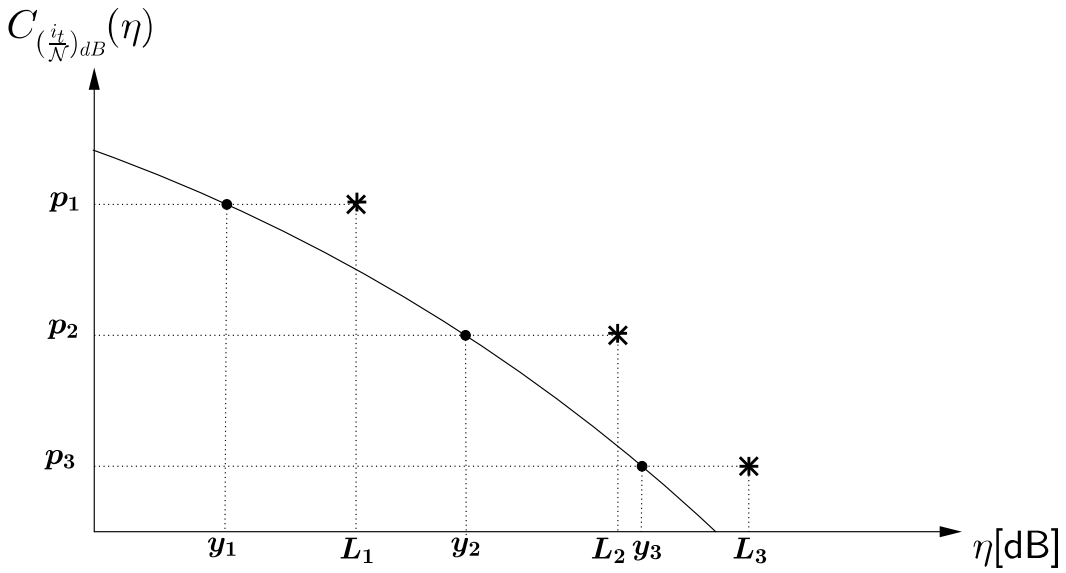

Figure 2.3: values y_ℓ that satisfy $C_{\left(\frac{i_t}{N}\right)_{dB}}(y_\ell) = p_\ell$

Let then μ_ℓ, be the margin with which (2-31) is satisfied, that is

$$\mu_\ell = L_\ell - y_\ell, \quad \ell = 1, 2, 3. \tag{2-34}$$

Note that a negative margin indicates that the corresponding criterion is not satisfied. Figure 2.4 illustrates a situation in which all margins are positive, meaning that all protection criteria are satisfied.

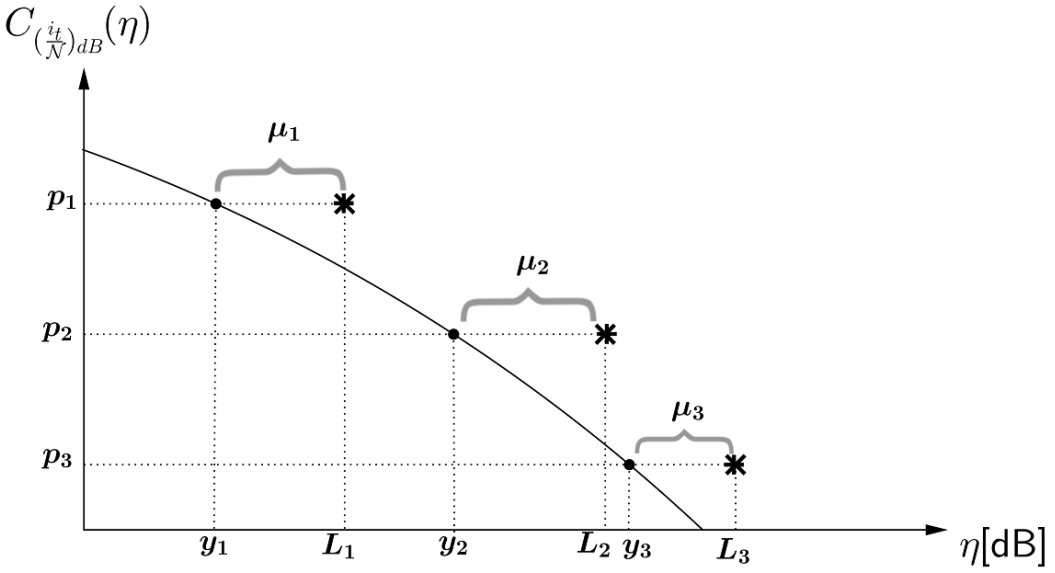

Figure 2.4: Margins μ_ℓ

Observe that different pointing directions of the FS receiving antenna will yield different cumulative distribution functions $C_{(\frac{i_t}{N})_{dB}}(\eta)$. Since, in this work, the elevation angle is considered to be constant and only the azimuth α varies, it is possible to obtain conditional cumulative distribution functions $C_{(\frac{i_t}{N})_{dB}|\alpha=A}(\eta)$, given $\alpha = A$, for different values of A. In this case, the interference to noise ratio levels $\{y_\ell,\ \ell = 1, 2, 3\}$ are dependent on α and so are the margins $\{\mu_\ell,\ \ell = 1, 2, 3\}$. Since, as indicated in Section 2.2, the azimuth α is being here considered as a random variable, the margins $\{\mu_\ell,\ \ell = 1, 2, 3\}$ are also random variables. Note that, given $\alpha = A$, the interference to noise ratio levels $\{y_\ell(A),\ \ell = 1, 2, 3\}$ can be determined by solving an equation equivalent to (2-33), that is,

$$C_{(\frac{i_t}{N})_{dB}|\alpha=A}(y_\ell(A)) = p_\ell, \quad \ell = 1, 2, 3. \tag{2-35}$$

The probability density function of the ℓ-th margin can be expressed as

$$p_{\mu_\ell}(M) = \int_{\Omega_\alpha} p_{\mu_\ell|\alpha=A}(M)\ p_\alpha(A)\ dA. \tag{2-36}$$

Note that, given $\alpha = A$, μ_ℓ equals $L_\ell - y_\ell(A)$ with probability 1, that is,

$$p_{\mu_\ell|\alpha=A}(M) = \delta(M - (L_\ell - y_\ell(A))). \tag{2-37}$$

As a consequence, (2-36) becomes

$$p_{\mu_\ell}(M) = \int_{\Omega_\alpha} \delta(M - (L_\ell - y_\ell(A)))\ p_\alpha(A)\ dA. \tag{2-38}$$

The probability distribution function of μ_ℓ is then given by

$$F_{\mu_\ell}(M) = P(\mu_\ell \leq M) = \int_{-\infty}^{M} \int_{\Omega_\alpha} \delta(v - (L_\ell - y_\ell(A)))\ p_\alpha(A)\ dA\ dv, \qquad (2\text{-}39)$$

or,

$$F_{\mu_\ell}(M) = P(\mu_\ell \leq M) = \int_{\Omega_\alpha} u(M - (L_\ell - y_\ell(A)))p_\alpha(A)dA. \qquad (2\text{-}40)$$

3
An Alternative Power-Flux Density Mask

In this chapter, the current Article 21 *pdf* mask for the 3.7-4.2 Gz Band is analysed and preliminary results on its adequacy to protect the Fixed Service without imposing undue constraints to non-GSO satellite systems are obtained. Also, a methodology to design *pfd* limiting masks is presented and used to produce a new *pfd* mask that would be an alternative to that in RR Article 21.

3.1
Current Power-Flux Density Mask: Preliminary Results

The current *pfd* limits in Table 21.4 of Article 21 of the Radio Regulations [2], applicable to non-GSO systems operating in the 3.4-4.2 GHz frequency band, expressed in dB(W/m^2), in a 1 MHz band, are given by

$$pfd(\delta, N_N, N_S) = \begin{cases} -138 - Y(N_N, N_S) & 0° < \delta < 5° \\ -138 - Y(N_N, N_S) + (12 + Y(N_N, N_S))\frac{\delta - 5}{20} & 5° \leq \delta < 25° \\ -126 & 25° \leq \delta, \end{cases} \tag{3-1}$$

where δ is the arrival angle at the earth surface and

$$Y(N_N, N_S) = \begin{cases} 0 & ; \quad \max(N_N, N_S) \leq 2 \\ 5\log(\max(N_N, N_S)) & ; \quad \max(N_N, N_S) > 2, \end{cases} \tag{3-2}$$

with N_N and N_S denoting the maximum number of space stations simultaneously transmitting on a co-frequency basis in the northern and southern hemispheres, respectively. According to Note 17 in Article 21 of the RR, these limits are supposed to be reviewed if the number of co-frequency non-geostationary systems brought into use and simultaneously operating in the same hemisphere is greater than five. This *pfd* mask is illustrated in Figure 3.1.

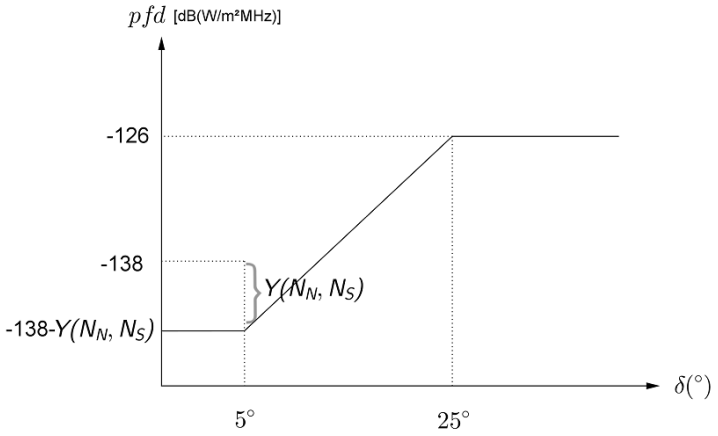

Figure 3.1: Table 21-4 of Radio Regulations, Power flux-density limit

Aiming to analyze this current Article 21 *pfd* mask, five different *Walker Delta type* satellite constellation structures were considered, since they are the most common type of non-GSO satellite constellation used, as indicated in Table 3.1.

Table 3.1: Technical characteristics of the considered systems

System	A	B	C	D	E
Altitude [km]	10352	1414	1400	1375	1200
Orbital plane inclination [degree]	55	52	52	84.7	87.9
Number of orbital planes	4	8	12	12	18
Number of satellites per plane	5	6	10	24	40
ΔM between adj planes [degree]	0	7.5	3	1.25	4.5
Plane spacing [degree]	90	45	30	15.36	10.2

In the analysis, the FS receiver characteristics in Table 3.2 were considered.

Table 3.2: FS receiver characteristics

Operating frequency f [Ghz]	4
Receiving antenna elevation ϵ [degree]	0
Receiving antenna azimuth α [degree]	0 to 360
Feeder losses L_{FS} [dB]	3
Antenna efficiency η	0.55
Noise level $\mathcal{N}$ [dB(W/MHz)]	-140
Antenna diameter D [meters]	3.0, 3.6 and 4.5
Location latitude θ_{FS} [degree]	0, 10, 20, 30 and 40

The radiation pattern considered for the receiving FS antenna was that in Recommendation ITU-R F.1245-1 for $D/\lambda \leq 100$ [18], that is,

$$G_{FS}(\gamma) = \begin{cases} G_{max} - 2.5\ 10^{-3}\ \left(\frac{D}{\lambda}\gamma\right)^2 & 0° < \gamma < \gamma_M \\ 39 - 5\log\frac{D}{\lambda} - 25\log(\gamma) & \gamma_M \leq \gamma < 48° \\ -3 - 5\log\frac{D}{\lambda} & 48° \leq \gamma \leq 180°, \end{cases} \tag{3-3}$$

where

$$G_{max} = 10\log\left(\eta\left(\frac{\pi D}{\lambda}\right)^2\right), \tag{3-4}$$

and

$$\gamma_M = \frac{20\lambda}{D}\sqrt{G_{max} - G_1}, \tag{3-5}$$

with

$$G_1 = 2 + 15\log\frac{D}{\lambda} \tag{3-6}$$

denoting the gain of the first side-lobe.

The following steps were performed to determine, for each of the five systems, the probability distribution function of the margin μ_ℓ in (2-40):

1. the conditional probability density function $p_{i_{agg}|\alpha=A}(I)$ of the aggregate interference due to a single non-GSO system, in (2-23), was determined for different azimuth values A. The integral in (2-23) was obtained by using the Analytical Method [15] and by using (3-1) and (3-2);

2. five identical co-frequency non-GSO systems were assumed to operate simultaneously and the conditional cumulative distribution function $C_{i_t|\alpha=A}(I)$ of the total aggregate interference due to all five systems was obtained using (2-28) and (2-27) with $K = 5$;

3. the conditional cumulative distribution function $C_{\left(\frac{i_t}{N}\right)_{dB}|\alpha=A}(I)$ of the interference to noise ratio was obtained using (2-30);

4. equation (2-35) was solved to determine the values of $\{y_\ell(A), \ell = 1, 2, 3\}$ for different values of A; the protection criteria used was the one defined in Recommendation ITU-R F.1495 [17];

5. finally, the probability distribution functions of the margins $\{\mu_\ell, \ell = 1, 2, 3\}$ were determined using (2-40).

Examples of the conditional cumulative distribution function $C_{\left(\frac{i_t}{N}\right)_{dB}|\alpha=A}(I)$, are ilustrated in figures 3.2 and 3.3 for non-GSO systems E and B, respectively. For reference purposes, the protection criteria in Recommendation ITU-R F.1495 are also shown in these figures (asterisks). In both figures, the azimuth α varies from 0° to 360°. The curves in Figure 3.2 were obtained for for $\theta_{FS} = 40°$, $D = 4.5$ meters while those in Figure 3.2 were obtained for for $\theta_{FS} = 20°$, $D = 3.6$ meters.

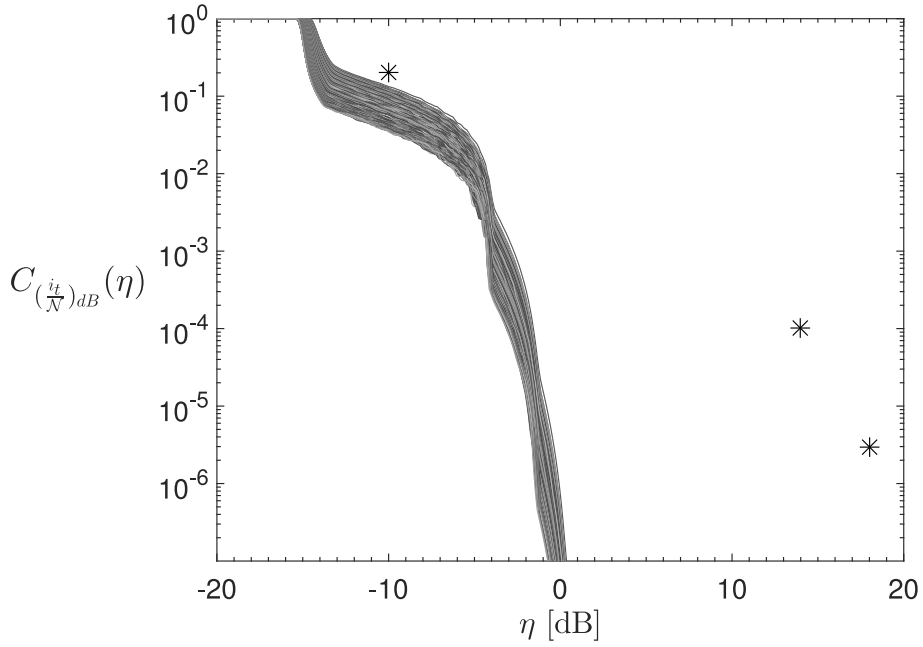

Figure 3.2: Cumulative distribution of the total interfering power produced by 5 systems of type E into a FS receiver located at $\theta_{FS} = 40°$ and with antenna diameter of $D = 4.5$ meters, for 180 different values of azimuth α.

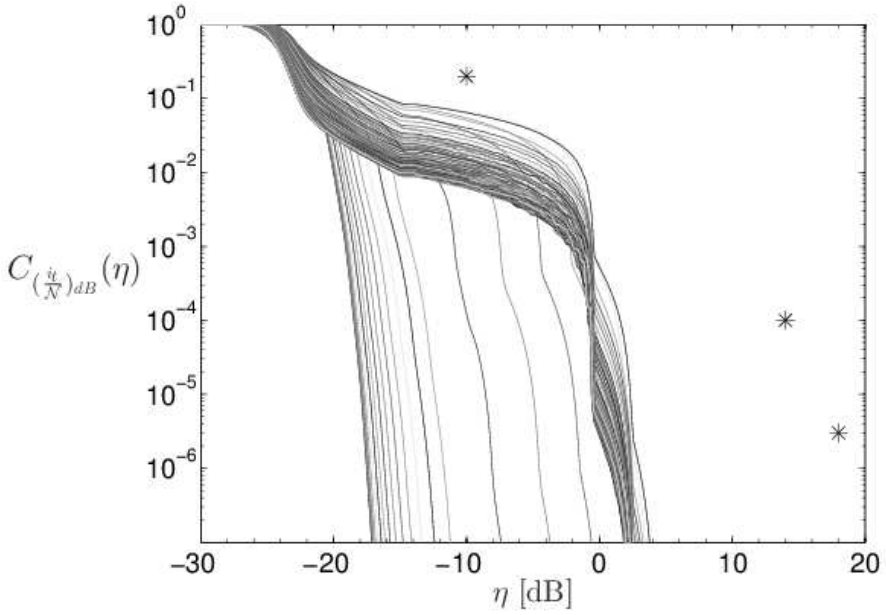

Figure 3.3: Cumulative distribution of the total interfering power produced by 5 systems of type B into a FS receiver located at $\theta_{FS} = 20°$ and with antenna diameter of $D = 3.6$ meters, for 180 different values of azimuth α.

For each of the satellite constellation structures in Table 3.1, the probability distribution function $F_\mu(M)$ of the interference margin μ_ℓ was determined

for $\ell = 1, 2, 3$, $\theta_{FS} = 0, \pm 10, \pm 20, \pm 30, \pm 40^{\circ}$ and $D = 3, 3.6, 4.5$ meters. It is important to note that, due to the symmetry of the *circular orbits Walker Delta constellation structure*, the interference results do not depend on the FS location longitude.

As an example, the results obtained for $\theta_{FS} = 10^{\circ}$ and $D = 3.6$ meters are shown in Figure 3.4. Note that the curves in Figure 3.4 indicate very large interference margin values (greater than 15 dB for the short-term criteria and greater than 10 dB for the long term criterion, except for system E). Large margins were also observed for different FS location latitudes and different FS receiving antenna diameters, indicating that the current Article 21 *pfd* mask is over protective and too much restrictive to most non-GSO satellite systems. A methodology to investigate new *pfd* masks is presented in Section 3.2.

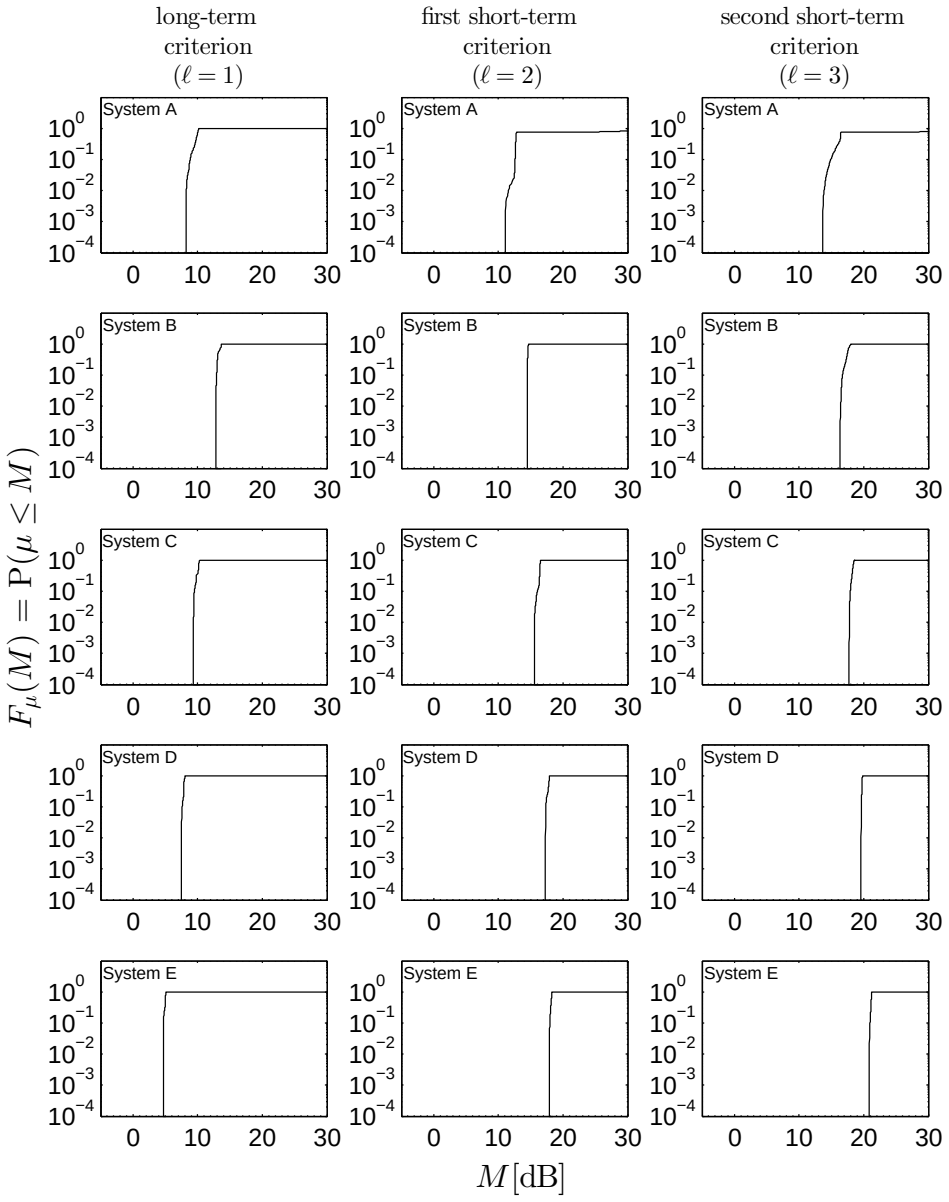

Figure 3.4: Probability distribution function of the interference margin μ_ℓ for a FS receiver located at latitude 10°N and FS antenna diameter 3.6 meters.

3.2
A Methodology to Design Power-Flux Density Masks

In this section, a methodology to design limiting *pfd* masks is presented and used in defining a new *pfd* mask that represents an alternative to the current Article 21 mask. The methodology considers the particular case of non-GSO satellite systems having constellation symmetry in the North and the South Hemispheres as, for example, those with a *Walker Delta* structure. In this case,

$$N_S = N_N = \frac{N}{2}, \tag{3-7}$$

and the current Article 21 *pfd* mask in (3-1) becomes

$$pfd(\delta, N) = \begin{cases} -138 - Y(N) & 0° < \delta < 5° \\ -138 - Y(N) + (12 + Y(N))\frac{\delta - 5}{20} & 5° \leq \delta < 25° \\ -126 & 25° \leq \delta, \end{cases} \tag{3-8}$$

with N denoting total number of satellites in the non-GSO system and

$$Y(N) = \begin{cases} 0 & ; \quad N \leq 4 \\ 5\log(\frac{N}{2}) & ; \quad N > 4. \end{cases} \tag{3-9}$$

At this point it is interesting to consider the Article 21 *pfd* mask applicable to GSO systems operating in the 3.4-4.2 GHz band, expressed in dB(W/m^2) in a 4 kHz bandwidth, given by

$$pfd(\delta) = \begin{cases} -152 & 0° < \delta < 5° \\ -152 + 0.5(\delta - 5) & 5° \leq \delta < 25° \\ -142 & 25° \leq \delta. \end{cases} \tag{3-10}$$

or equivalently, in dB(W/m^2) in a 1 MHz bandwidth,

$$pfd(\delta) = \begin{cases} -128 & 0° < \delta < 5° \\ -128 + 0.5(\delta - 5) & 5° \leq \delta < 25° \\ -118 & 25° \leq \delta. \end{cases} \tag{3-11}$$

Figure 3.5 illustrates the current Article 21 *pfd* masks for GSO networks (see 3-8)) and for non-GSO systems with 1 and 100 satellites (see (3-8)).

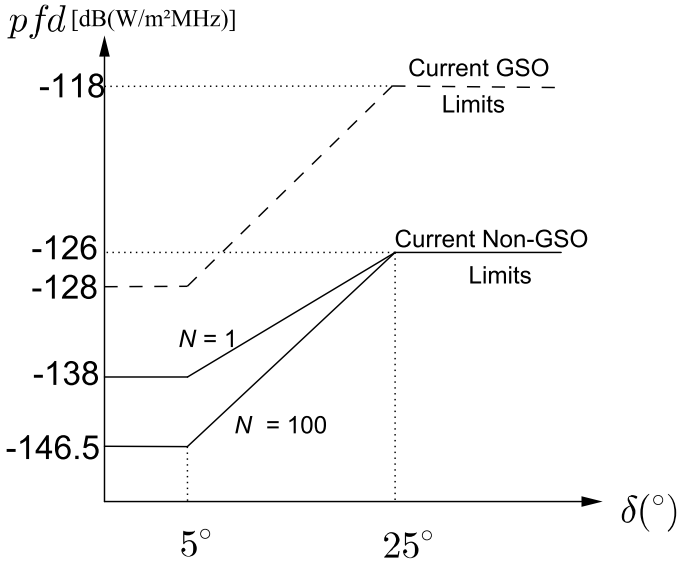

Figure 3.5: Current limits for the GSO and non-GSO satellite systems

For compatibility purposes, it would be desirable that the new non-GSO mask approaches the GSO mask when $N = 1$ (one non-GSO satellite in the

system). As shown in Figure 3.5, this does not happen with the current Article 21 masks.

It is expected that the maximum *pfd* limit for each individual satellite in a non-GSO system be dependent on the number of satellites in the constellation. The limit should be lower for non-GSO systems with a larger number of satellites, so that the aggregate interference to noise ratio at the FS victim receiver, due to all visible satellites, satisfy the FS protection criterion. In this respect, the term $Y(N)$ in the current Article 21 *pfd* limits guarantees that non-GSO systems with a higher number of operating satellites are subjected to a higher constraint on individual satellite transmit powers. More specifically, as shown in Figure 3.5, $Y(N)$ has effects on the maximum *pfd* values for arrival angles less or equal to 25°.

This makes sense for non-GSO systems with a low number of satellites, as the strongest interference entries occur for satellites located within the main beam of the FS receiving antenna, which usually points to a low elevation angle (see Figure 3.6). However, for non-GSO systems with a large number of satellites as, for example, systems D and E in Table 3.1, it is possible that the large number of satellites located within the side-lobe region of the FS receiving antenna (see Figure 3.7) be responsible for a non negligible amount of interference. In this case, it seems reasonable to consider an additional term $X(N)$ that has influence on the *pfd* limits for arrival angles greater than 25°.

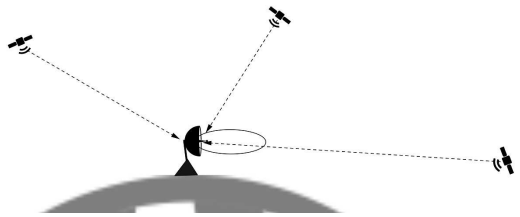

Figure 3.6: System with few satellites

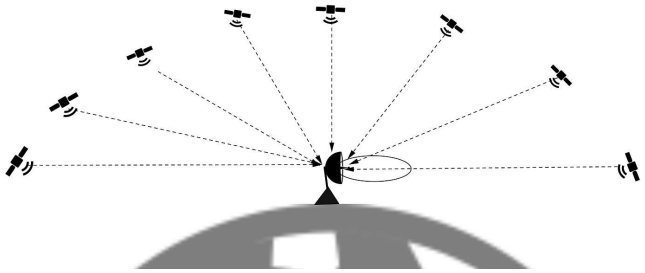

Figure 3.7: System with many satellites

Hence, a new mask is proposed with two limitation factors, $Y(N)$ and $X(N)$, for arrival angles below 5° and above 25°, respectively. In this case, the

pfd mask has the form

$$pfd(\delta, N) = \begin{cases} -(A + Y(N)) & 0° < \delta < 5° \\ -(A + Y(N)) + (Y(N) - X(N) + A - B)\ \frac{\delta - 5}{20} & 5° \leq \delta < 25° \\ -(B + X(N)) & 25° \leq \delta. \end{cases} \tag{3-12}$$

with $X(N)$ and $Y(N)$ assumed to be zero for $N = 1$.

3.3 Proposed Alternative Power-Flux Density Mask

The values of A and B in (3-12) are determined so that, for $N = 1$, (3-12) is compatible with (3-11). The proposed mask then becomes

$$pfd(\delta, N) = \begin{cases} -(128 + Y(N)) & 0° < \delta < 5° \\ -(128 + Y(N)) + (Y(N) - X(N) + 10)\ \frac{\delta - 5}{20} & 5° \leq \delta < 25° \\ -(118 + X(N)) & 25° \leq \delta. \end{cases} \tag{3-13}$$

This mask is illustrated in Figure 3.8.

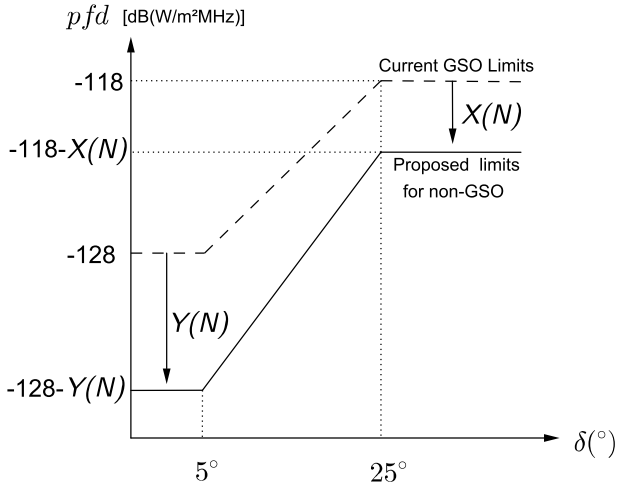

Figure 3.8: Proposed Limits for non-GSO systems and current limits for GSO systems

As in the current Article 21 mask for non-GSO systems operating in the 3.4-4.2 GHz band, we have considered a logarithm shape for $Y(N)$, that is,

$$Y(N) = a_y \log \frac{N}{b_y}. \tag{3-14}$$

The same was assumed for $X(N)$, that is,

$$X(N) = a_x \log \frac{N}{b_x}. \tag{3-15}$$

The following procedure was used to determine the values of a_x, a_y, b_x, b_y in (3-14) and (3-15):

Firstly, the worst-case scenario in terms of the FS receiver latitude θ and the azimuth α of its receiving antenna was determined for each of the systems in Table 3.1. This was done by considering the current limits in Table 21.4 of Article 21 of the Radio Regulations and by determining the probability distribution functions of the margins μ_ℓ using the steps described in Section 3.1. These steps were repeated for 9 different latitudes ($\theta = 0°, \pm10°, \pm20°, \pm30°$ and $\pm40°$) and for azimuths α varying from 0° to 360°. The worst-case scenario for each non-GSO system was defined by the latitude and azimuth of the FS receiving antenna which yielded the strongest interferences, or equivalently, the smallest margins μ_ℓ. These scenarios are presented in Table 3.3.

Table 3.3: Worst-case scenarios for each non-GSO system

System	Worst θ	Worst α
A	10°	40°
B	40°	60°
C	40°	10°
D	40°	10°
E	40°	0°

Secondly, for each of these worst-case scenarios, many values of $Y(N)$ and $X(N)$ were jointly tested. For each of the considered non-GSO systems, the smallest values of $X(N)$ and $Y(N)$ that allowed for resulting margins close to zero (small positive margins or very small negative margins) were determined. These values are here called *reference values*. In other words, the choice was based on the highest values of power that would yield acceptable interferences. In this way, both the satellite non-GSO systems and the victim fixed service would benefit, since the first would be allowed to operate with higher energy and the second would still be protected from interference. In other words, the FS receiver would be adequately protected from interference without imposing undue constraints to the non-GSO satellite system. The obtained reference values for $X(N)$ and $Y(N)$ are presented in Table 3.4.

Table 3.4: Reference values of $X(N)$ and $Y(N)$ for each system

System	i	N	X_{ref}	Y_{ref}
A	1	20	0.0	4.0
B	2	48	0.0	6.0
C	3	120	2.8	12.0
D	4	288	4.1	15.8
E	5	720	8.1	21.9

Lastly, the values of the parameters a_x, b_x, a_y, b_y were determined so that the curves in (3-14) and (3-15) adequately fit the reference values in Table 3.4. The Least Squares fitting method was used, meaning that the values of (a_y, b_y) and (a_x, b_x) were determined so that the objective functions

$$\epsilon_y(a_y, b_y) = \frac{1}{5}\sum_{i=1}^{5}\left(a_y \log\frac{N_i}{b_y} - Y_{ref_i}\right)^2 \tag{3-16}$$

and

$$\epsilon_x(a_x, b_x) = \frac{1}{4}\sum_{i=2}^{5}\left(a_x \log\frac{N_i}{b_x} - X_{ref_i}\right)^2 \tag{3-17}$$

were individually minimized. This procedure led to $a_x = 6.5591$, $b_x = 49.8378$, $a_y = 11.7315$ and $b_y = 11.4253$.

Considering that integer numbers would be preferable in a regulatory text, an approximation to nearest pair of integers was done. Table 3.5 presents the four possible neighbouring integer pairs for the optimum values of a_y and b_y. Similarly, Table 3.6 presents the four possible neighbouring integer pairs for the optimum values of a_x and b_x. The integer pairs corresponding to the lowest values of ϵ_y and ϵ_x were chosen, leading to $a_y = 12$, $b_y = 12$, $a_x = 7$ and $b_x = 50$. The resulting fitting curves, along with the respective reference points are illustrated in figures 3.9 and 3.10.

Table 3.5: Calculated ϵ_y for the approximations

a_y	b_y	ϵ_y $[dB(W/m^2MHz)^2]$
11.7315 (least squares)	11.4253 (least squares)	0.8153
12	12	0.8374
12	11	1.0589
11	12	1.9358
11	11	1.2947

Table 3.6: Calculated ϵ_x for the approximations

a_x	b_x	ϵ_x $[dB(W/m^2MHz)^2]$
6.5591 (least squares)	49.8378 (least squares)	0.2868
7	50	0.3826
6	50	0.4541
7	49	0.4161
6	49	0.4223

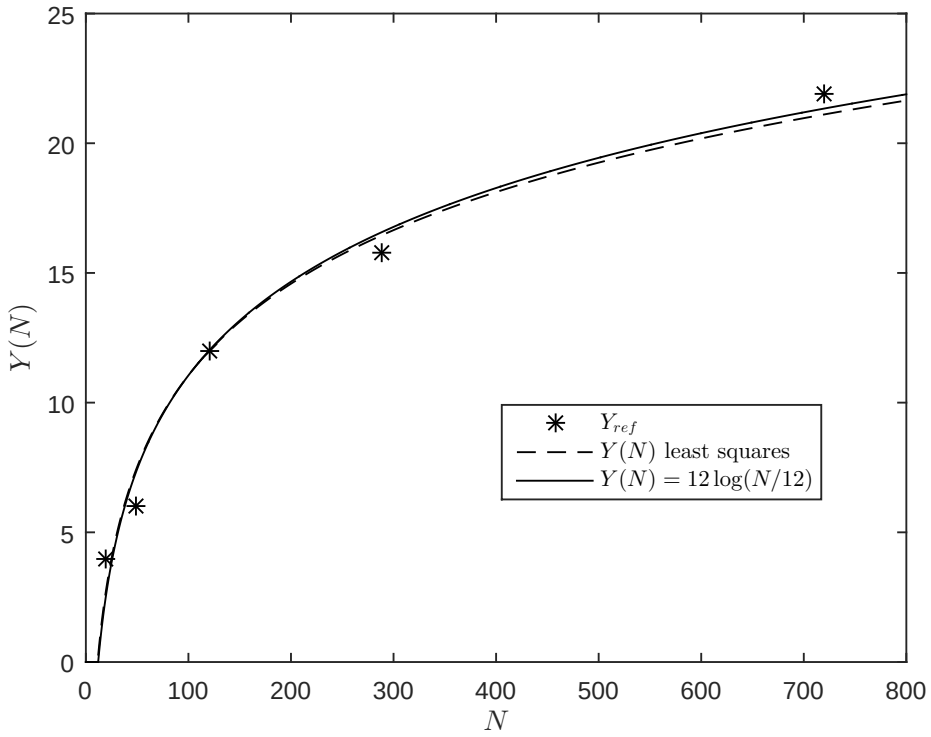

Figure 3.9: Best fit for $Y(N)$

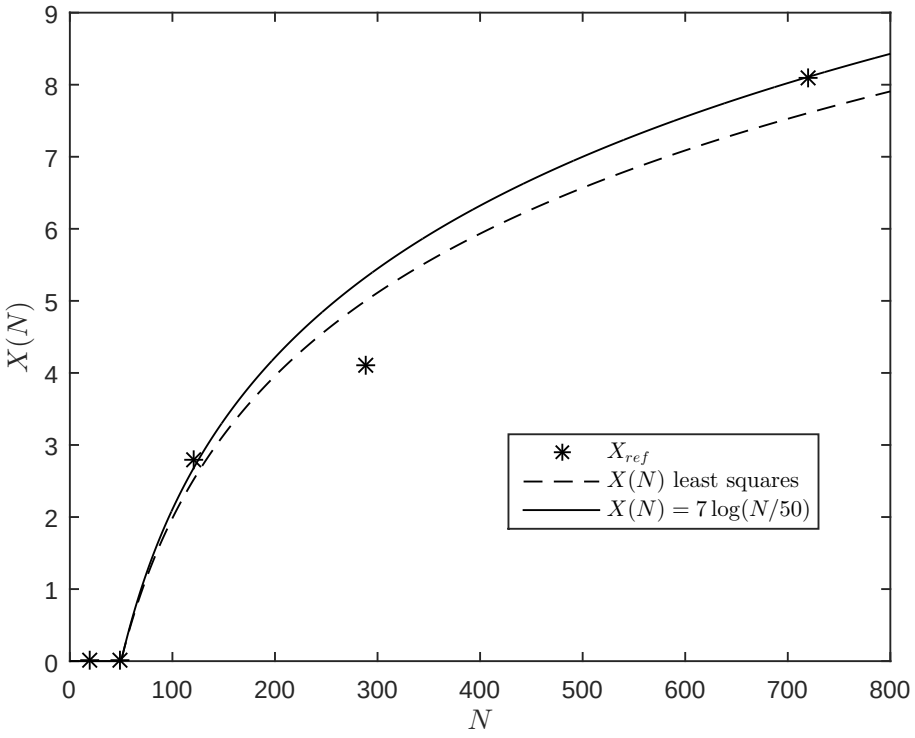

Figure 3.10: Best fit for $X(N)$

As a result, the proposed pfd limits, applicable to non-GSO systems with circular orbit (Walker Delta constellations) operating in the 3.4-4.2 GHz frequency band, expressed in dB(W/m^2), in a 1 MHz band, are given by

$$pfd(\delta, N) = \begin{cases} -(128 + Y(N)) & 0° < \delta < 5° \\ -(128 + Y(N)) + (Y(N) - X(N) + 10)\frac{\delta - 5}{20} & 5° \leq \delta < 25° \\ -(118 + X(N)) & 25° \leq \delta, \end{cases} \tag{3-18}$$

where

$$Y(N) = \begin{cases} 0 & N < 12 \\ 12\log\frac{N}{12} & N > 12, \end{cases} \tag{3-19}$$

and

$$X(N) = \begin{cases} 0 & N < 50 \\ 7\log\frac{N}{50} & N > 50. \end{cases} \tag{3-20}$$

It is important to note that the pfd mask in (3-18) is supposed to protect FS receivers from interference generated by up to 5 non-GSO satellite systems. Also, constellations with types different than that of the Walker Delta would require studies aiming for another pfd mask, specific to them, as it already happens with the other frequency bands in the Article 21 of Radio Regulations.

Finally, the pfd mask in (3-18) is illustrated in Figure 3.11 for different values of the non-GSO constellation size N.

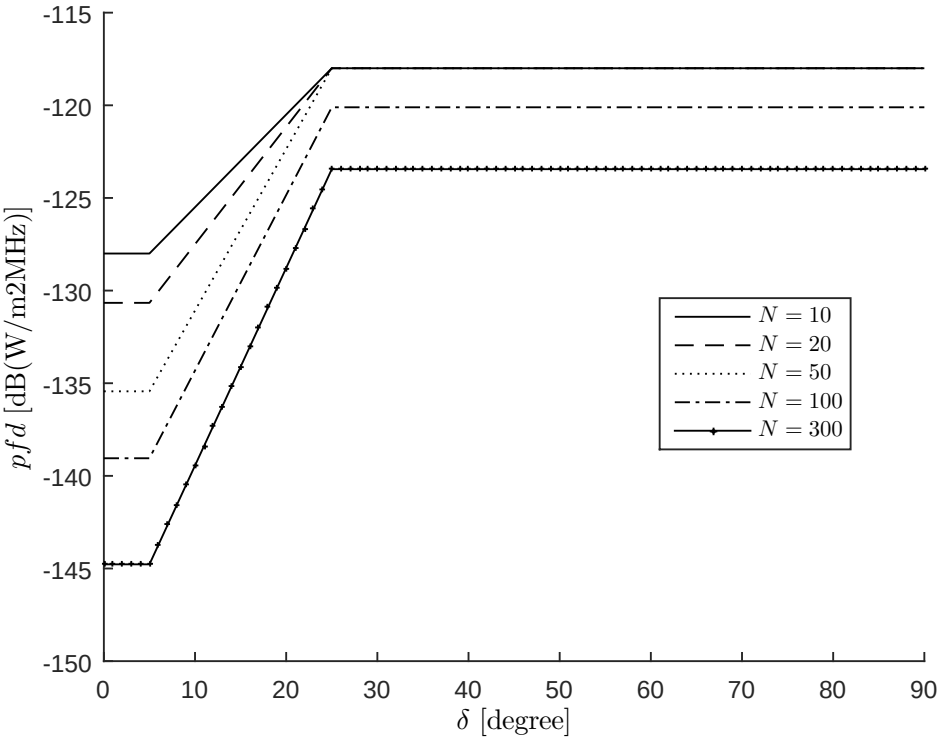

Figure 3.11: The proposed *pfd* mask for different values of the non-GSO constellation size N.

4
Analysis of the Proposed Power-Flux Density Limits

In this chapter, the protection given to FS receivers by the proposed *pfd* mask in (3-18) is evaluated. The basis for the analysis are the margins $\{\mu_\ell, \ell = 1, 2, 3\}$ of the $i_t/\mathcal{N}$ ratio with respect to the interference criteria in Recommendation ITU-R F.1495 (see Section 2.4), as defined by (2-34) and (2-33).

Considering the FS receiving antenna has a zero degree elevation angle and an azimuth characterized by a random variable uniformly distributed in the interval $(0°, 360°]$, the probability distribution function of the $i_t/\mathcal{N}$ margin μ_ℓ is determined for different FS receiving antenna diameters and different FS location latitudes. More specifically, FS receiving antennas with 3.0, 3.6 and 4.5 meters diameters and FS receivers located at latitude $0°, \pm 10°, \pm 20°, \pm 30°$ and $\pm 40°$ were considered. It is important to note that, due to the symmetry of the *circular orbits Walker Delta constellation structure*, the interference results do not depend on the FS location longitude.

The results corresponding to each of the antenna diameters are presented in sections 4.1, 4.2, and 4.3, respectively. In these sections, scenarios involving the non-GSO satellite systems in 3.1 were analyzed and the conditional cumulative distribution function $C_{i_t/\mathcal{N}|\alpha=A}(I)$ of the of the $i_t/\mathcal{N}$ ratio was determined taking into account the aggregate interference generated by 5 identical non-GSO systems. In determining these cumulative distribution functions, the Analytical Method in [15] was used. Here, the Analytical Method was implemented using the modifications suggested in [19], for a faster and simpler computation that takes advantages of existing symmetries in the problem. In all scenarios, the parameters in Table 3.2 and the receiving antenna radiation pattern in (3-3) to (3-6) were considered for the FS receiver.

4.1
FS receiving antenna with 3.0 meters diameter

In this section, the probability distribution functions of the $i_t/\mathcal{N}$ margins $\{\mu_\ell, \ell = 1, 2, 3\}$ were determined for the non-GSO constellations in Table 3.1. Figures 4.1 to 4.5 present, respectively, the results obtained for FS location latitudes equal to $0°, \pm 10°, \pm 20°, \pm 30°$ and $\pm 40°$. For comparison purposes,

the results corresponding to the current RR Article 21 *pfd* mask are also shown in these figures.

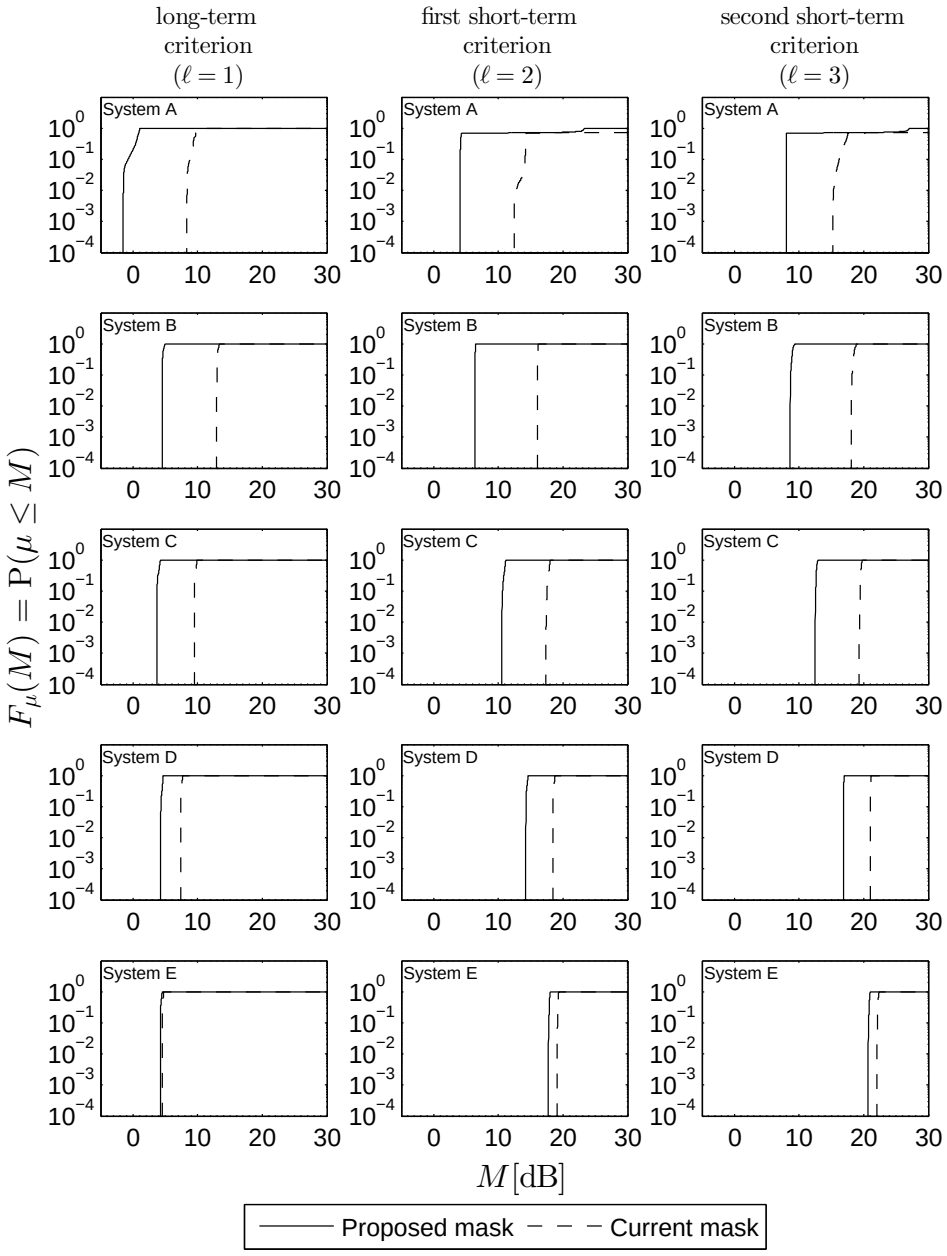

Figure 4.1: Probability distribution function of the interference margin μ_ℓ for a FS receiver located at latitude 0° and FS antenna diameter 3 meters.

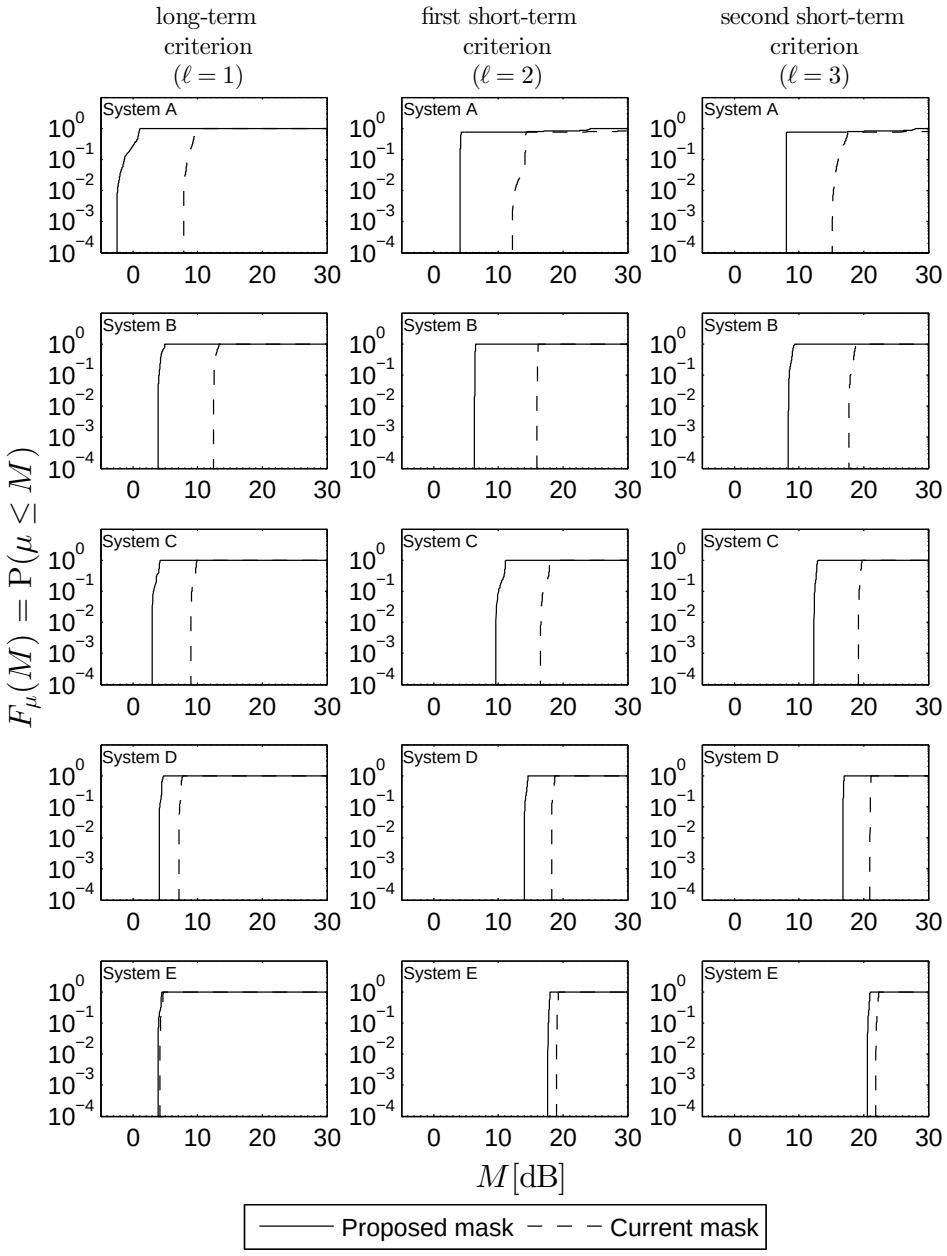

Figure 4.2: Probability distribution function of the interference margin μ_ℓ for a FS receiver located at latitude $\pm 10^\circ$ and FS antenna diameter 3 meters.

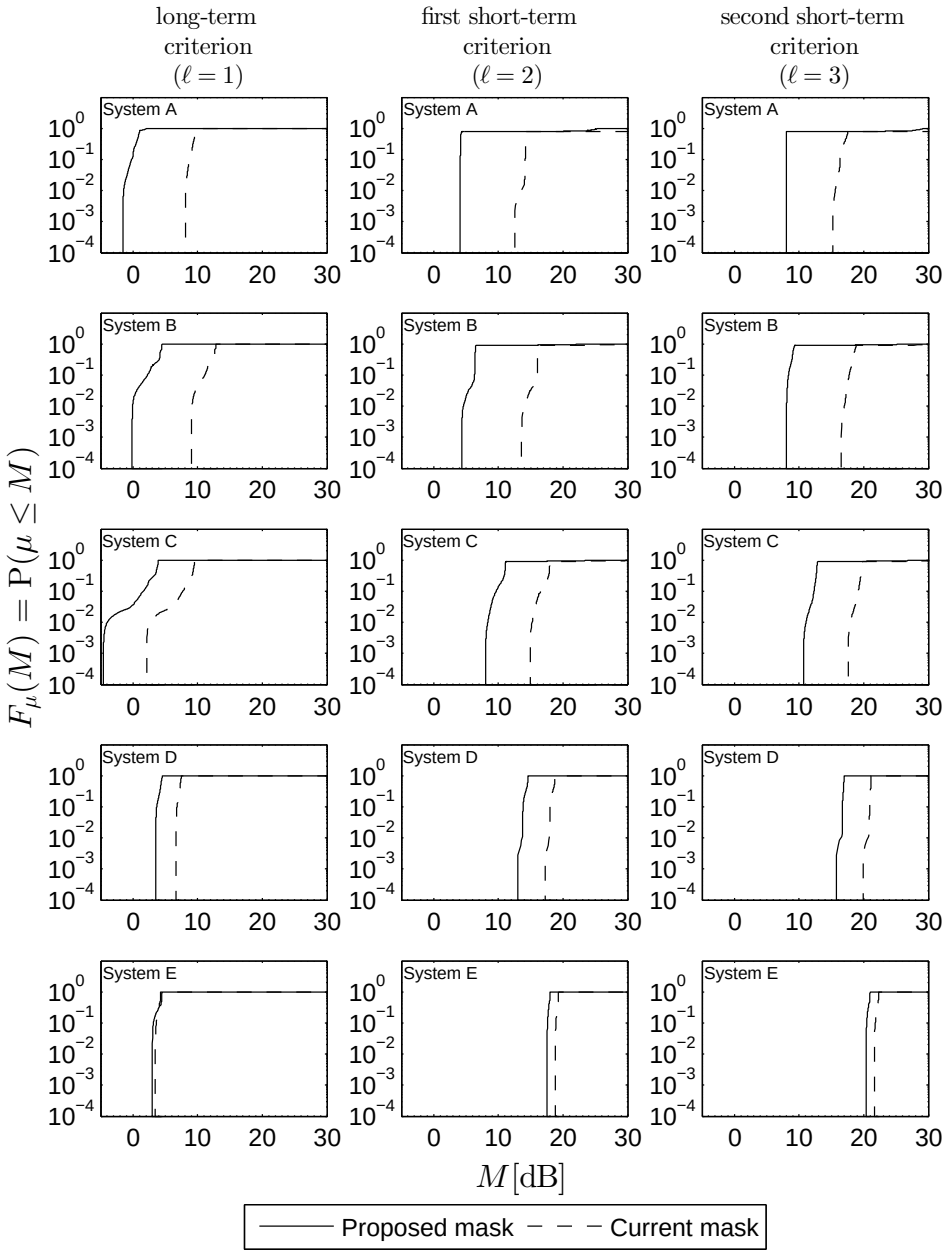

Figure 4.3: Probability distribution function of the interference margin μ_ℓ for a FS receiver located at latitude $\pm 20^\circ$ and FS antenna diameter 3 meters.

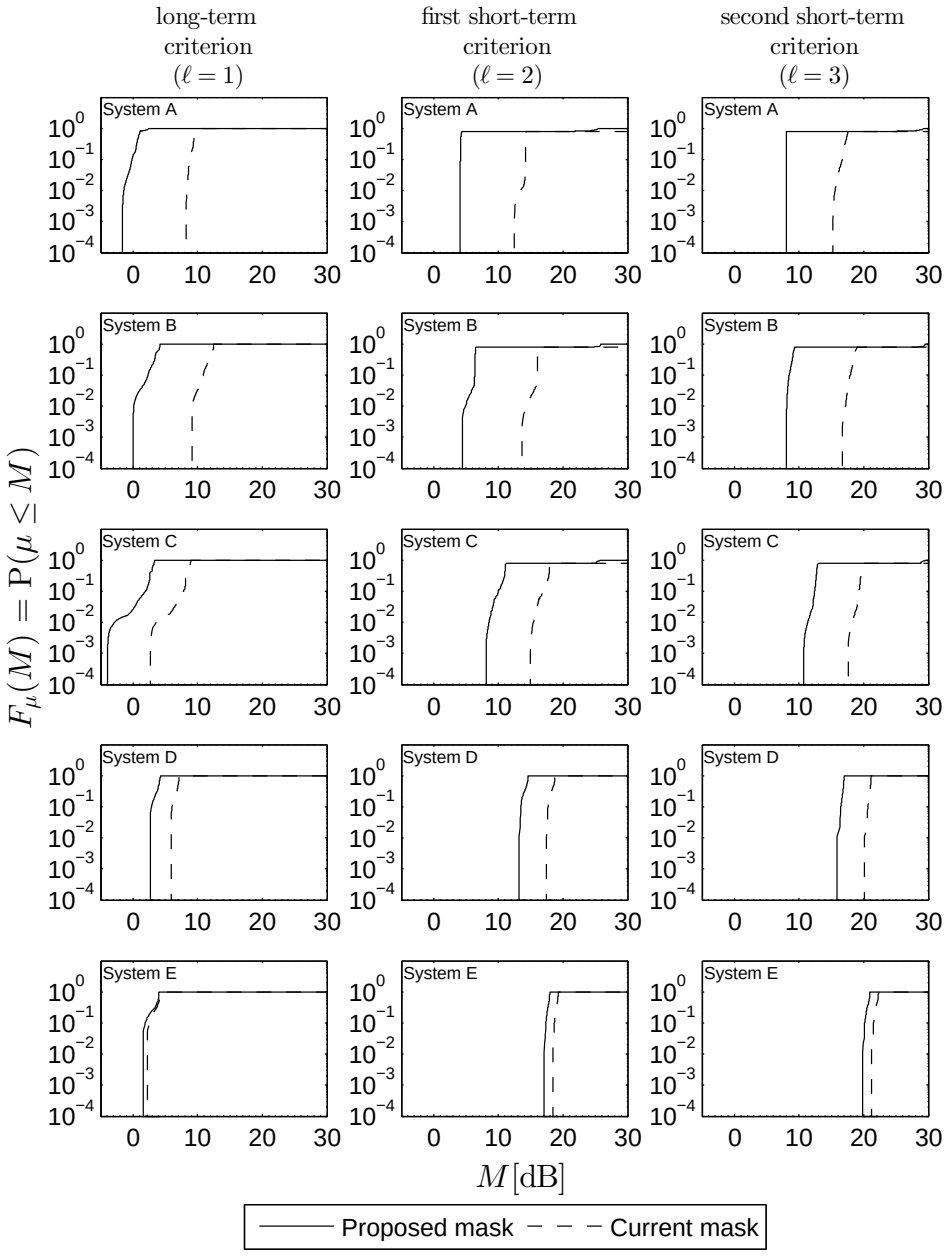

Figure 4.4: Probability distribution function of the interference margin μ_ℓ for a FS receiver located at latitude $\pm 30^\circ$ and FS antenna diameter 3 meters.

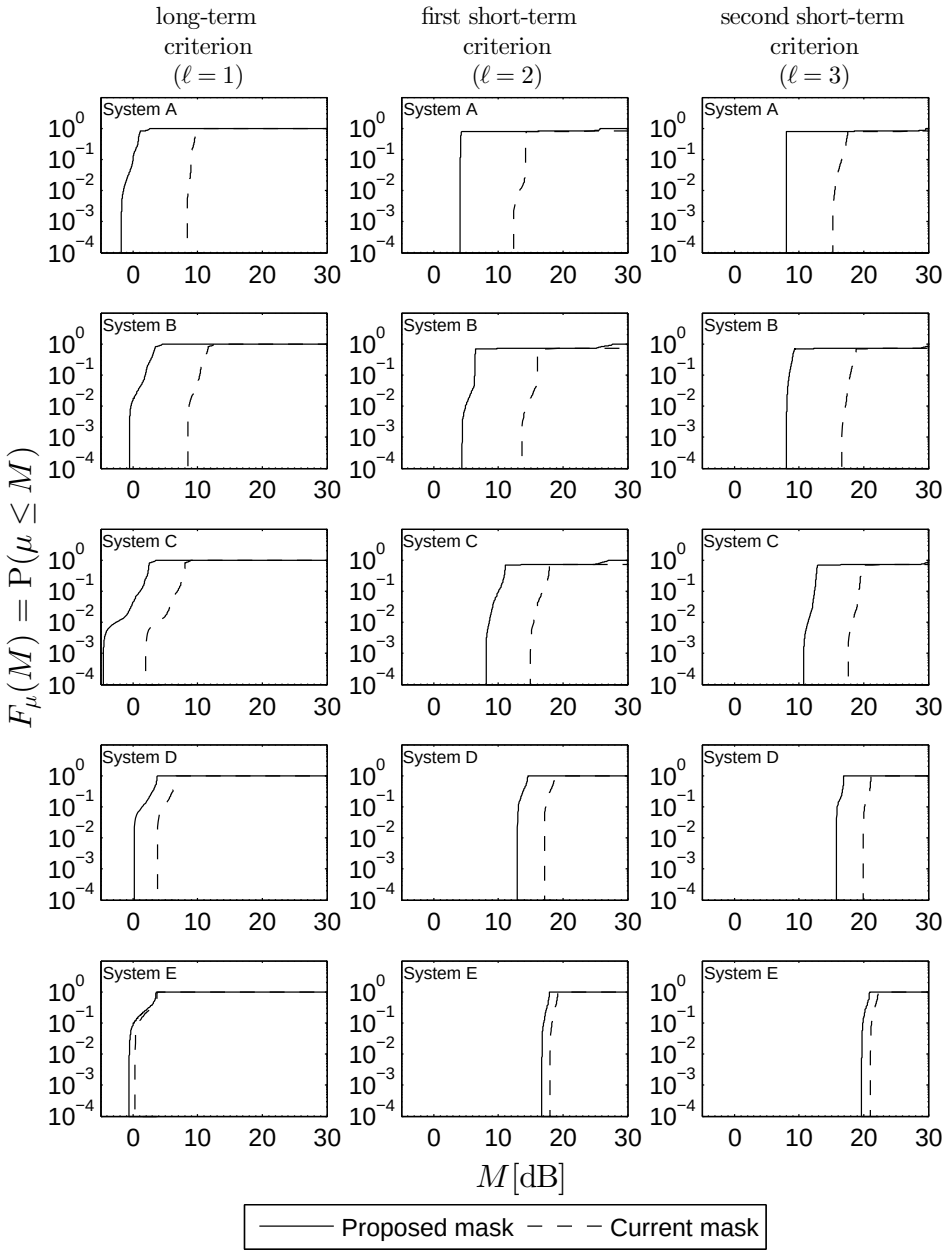

Figure 4.5: Probability distribution function of the interference margin μ_ℓ for a FS receiver located at latitude $\pm 40°$ and FS antenna diameter 3 meters.

For a better understanding of the results in figures 4.1 to 4.5, let M_p be the margin value exceeded with probability p, that is,

$$P(\mu_\ell > M_p) = p \tag{4-1}$$

This means that the chances of having an FS receiving antenna azimuth in which the margin μ_ℓ is less than or equal to M_p is equal to $1 - p$, or,

$$P(\mu_\ell \leq M_p) = 1 - p \tag{4-2}$$

Let then ΔM_p be defined as

$$\Delta M_p = M_p^{cur} - M_p^{prop} \tag{4-3}$$

with M_p^{cur} and M_p^{prop} denoting, respectively, the values of M_p corresponding to the current (RR-Art. 21) and the proposed *pfd* masks. Note that the value of ΔM_p reflects how much the proposed mask is less restrictive to non-GSO systems than the current mask. The average value of ΔM_p with respect to all considered FS latitudes ($0°, \pm 10°, \pm 20°, \pm 30°, \pm 40°$) is here denoted by ΔM_p^{avg}.

Another parameter of interest would be the smallest value of M_p (with respect to all considered FS latitudes) associated with the proposed *pfd* mask. This indicates how negative M_p can be if the proposed mask is used. Note that, due to some of the worst case conditions considered in the interference calculation (for example the assumption that all satellites in the constellation produce the maximum allowed power flux-density at the Earth's surface and the use of a reference antenna radiation pattern for the FS receiving antenna which do not reflect the oscillatory characteristics of the antenna sidelobe gains) it is not unreasonable to eventually have small negative $i/\mathcal{N}$ margins.

The values of M_p, ΔM_p^{avg} and M_p^{min} obtained for the current and the proposed *pfd* masks are shown in tables 4.1 and 4.2 for $p = 0.999$ and $p = 0.99$, respectively.

Table 4.1: Margin Levels (dB) exceeded with probability 0.999

FS receiver antenna diameter: 3m													
FS latitude		0°		±10°		±20°		±30°		±40°			
pfd mask		cur.	prop.	cur.	prop.	cur.	prop.	cur.	prop.	cur.	prop.	$\Delta M_{0.999}^{avg}$	$M_{0.999}^{min}$
	ℓ=1	8.4	-1.5	7.8	-2.5	8.1	-1.5	8.2	-1.6	8.4	-1.8	10.0	-2.5
System A	2	12.4	4.1	12.2	4.1	12.5	4.1	12.4	4.1	12.4	4.1	8.3	4.1
	3	15.2	8.1	15.2	8.1	15.3	8.1	15.2	8.1	15.2	8.1	7.2	8.1
	1	12.9	4.5	12.5	3.9	9.1	-0.1	9.1	0.0	8.5	-0.5	8.9	-0.5
System B	2	16.0	6.4	16.0	6.3	13.6	4.4	13.7	4.4	13.6	4.4	9.4	4.4
	3	18.0	8.6	17.7	8.3	16.5	8.1	16.7	8.1	16.6	8.1	8.9	8.1
	1	9.5	3.7	9.0	3.0	2.1	-4.6	2.7	-3.9	1.9	-4.6	6.3	-4.6
System C	2	17.3	10.5	16.5	9.6	14.9	8.0	15.0	8.1	15.0	8.1	6.9	8.0
	3	19.3	12.4	19.2	12.3	17.6	10.7	17.6	10.7	17.6	10.7	6.9	10.7
	1	7.3	4.3	7.1	4.0	6.7	3.5	5.9	2.7	3.8	0.2	3.2	0.2
System D	2	18.4	14.2	18.2	14.0	17.2	13.0	17.5	13.2	17.1	13.0	4.2	13.0
	3	21.0	16.8	21.0	16.8	20.0	15.8	20.1	15.9	19.9	15.7	4.2	15.7
	1	4.5	4.2	4.2	3.8	3.4	2.9	2.2	1.6	0.3	-0.6	0.5	-0.6
System E	2	19.1	17.7	19.0	17.6	18.8	17.5	18.4	17.1	18.0	16.7	1.3	16.7
	3	22.0	20.7	21.9	20.5	21.7	20.3	21.2	19.9	21.0	19.7	1.3	19.7

Table 4.2: Margin Levels (dB) exceeded with probability 0.99

FS receiver antenna diameter: 3m													
FS latitude		0°		±10°		±20°		±30°		±40°			
pfd mask		cur.	prop.	cur.	prop.	cur.	prop.	cur.	prop.	cur.	prop.	$\Delta M_{0.99}^{avg}$	$M_{0.99}^{min}$
	ℓ=1	8.4	-1.5	7.9	-2.4	8.2	-1.4	8.3	-1.4	8.6	-1.5	9.9	-2.4
System A	2	12.7	4.1	12.5	4.1	13.5	4.1	13.4	4.1	13.3	4.1	9.0	4.1
	3	15.4	8.1	15.3	8.1	15.6	8.1	15.6	8.1	15.5	8.1	7.4	8.1
	1	13.0	4.5	12.5	3.9	9.1	-0.1	9.2	0.1	8.7	-0.3	8.9	-0.3
System B	2	16.0	6.4	16.0	6.3	14.1	4.6	14.4	4.9	14.5	4.9	9.6	4.6
	3	18.1	8.6	17.7	8.4	17.0	8.1	17.2	8.1	17.2	8.1	9.2	8.1
	1	9.5	3.7	9.0	3.0	2.6	-4.0	3.6	-2.8	3.5	-2.6	6.2	-4.0
System C	2	17.4	10.5	16.6	9.6	15.2	8.4	15.4	8.6	15.5	8.6	6.9	8.4
	3	19.4	12.4	19.2	12.3	18.0	11.1	18.2	11.3	18.3	11.4	6.9	11.1
	1	7.3	4.3	7.1	4.0	6.7	3.5	5.9	2.7	3.8	0.2	3.2	0.2
System D	2	18.4	14.2	18.2	14.0	17.9	13.7	17.5	13.2	17.1	13.0	4.2	13.0
	3	21.0	16.8	21.0	16.8	20.6	16.5	20.1	15.9	19.9	15.7	4.2	15.7
	1	4.5	4.2	4.2	3.8	3.4	2.9	2.2	1.6	0.3	-0.6	0.5	-0.6
System E	2	19.1	17.7	19.0	17.6	18.8	17.5	18.4	17.1	18.0	16.8	1.3	16.8
	3	22.0	20.7	21.9	20.5	21.7	20.3	21.2	19.9	21.0	19.7	1.3	19.7

As indicated before, due to some of the worst case conditions considered in the interference calculation, negative margins around -2.0 dB, as those shown in tables 4.1 and 4.2 for System A, are acceptable.

For the system C and the long-term protection criteria ($\ell = 1$), however, the margins levels exceeded with probability 0.99 and 0.999 for the proposed mask, in the latitudes ±40° and ±20°, might seem too negative.

For the ±40° latitude, the margin levels exceeded with probabilities 0.99 and 0.999 are -2.6 dB and -4.6 dB, respectively (tables 4.1 and 4.2). However, as can be seen in Figure 4.5, the margin level exceeded with probabilities 0.98 is -0.8 dB and the probability to have it positive is 96%.

For the ±20° latitude, the margin levels exceeded with probabilities 0.99 and 0.999 are -4 dB and -4.6 dB, respectively (tables 4.1 and 4.2). However, as can be seen in Figure 4.3, the margin level exceeded with probabilities 0.98 is -2.3 dB and the probability that the margin is positive is also 96%. This means that the negative values for both cases are rare and thus acceptable.

For every other cases, the margins levels are either positive or slightly negative. It is important to note that the average margin differences ΔM_p^{avg} between the two considered masks are higher for systems with a low number of satellites. For systema with a high number of satellites, as System E ($N = 720$), for instance, the values of ΔM_p^{avg} are small. This means the current mask is

already appropriate for systems with a high number of satellites. However, for the other systems considered, it is too restrictive. It is also interesting to note that the long-term criterion ($\ell = 1$) is the one that limits the satellite transmitting power. In general, the values of M_p^{min} for the long-term criterion are all very close to zero, whereas for the other criteria ($\ell = 2, 3$) the margins are considerably positive.

4.2
FS receiving antenna with 3.6 meters diameter

Again, in this section, the probability distribution functions of the $i_t/\mathcal{N}$ margins $\{\mu_\ell, \ell = 1, 2, 3\}$ were determined for the non-GSO constellations in Table 3.1. Figures 4.6 to 4.10 present, respectively, the results obtained for FS location latitudes equal to $0°, \pm 10°, \pm 20°, \pm 30°$ and $\pm 40°$. For comparison purposes, the results corresponding to the current RR Article 21 *pfd* mask are also shown in these figures.

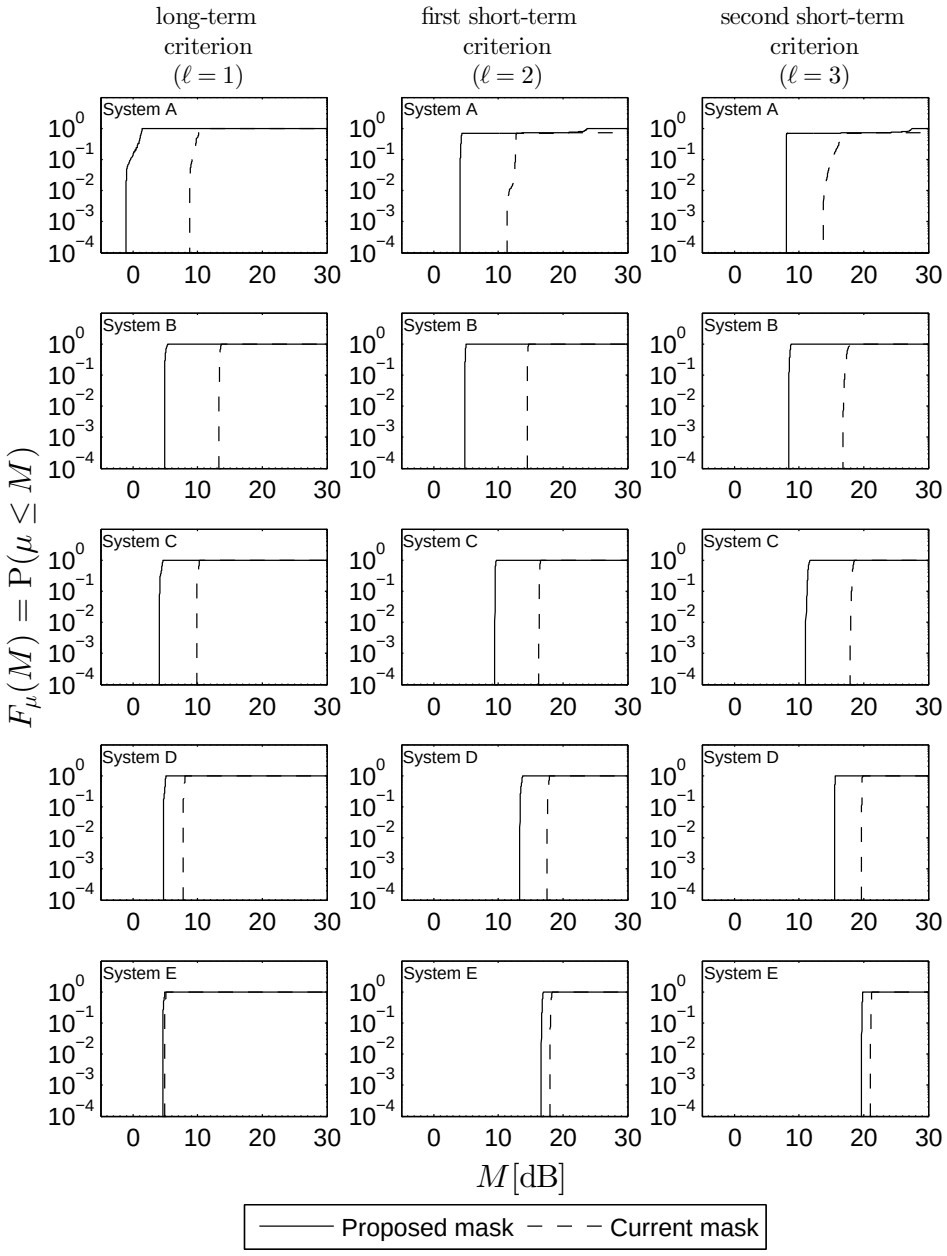

Figure 4.6: Probability distribution function of the interference margin μ_ℓ for a FS receiver located at latitude 0° and FS antenna diameter 3.6 meters.

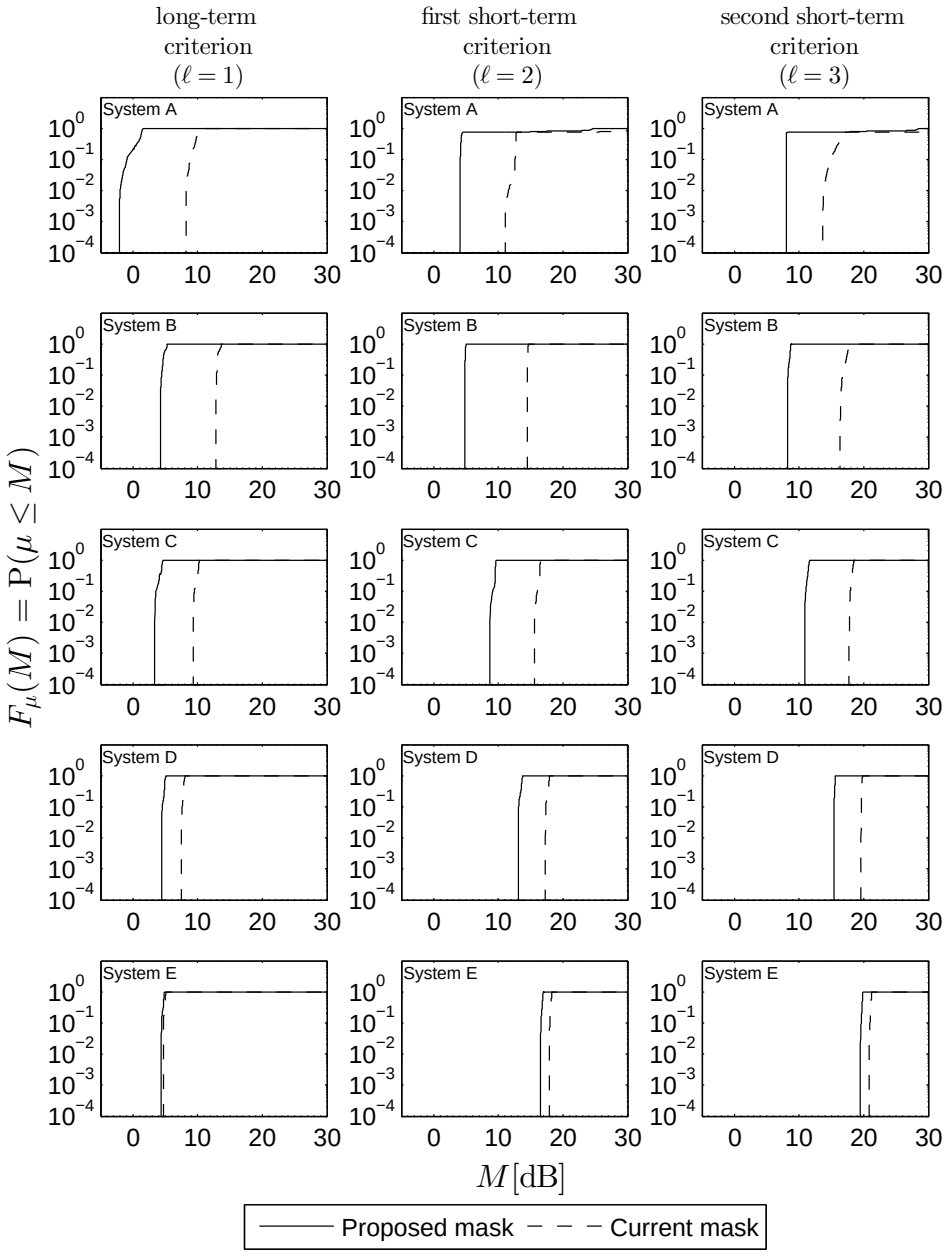

Figure 4.7: Probability distribution function of the interference margin μ_ℓ for a FS receiver located at latitude $\pm 10^\circ$ and FS antenna diameter 3.6 meters.

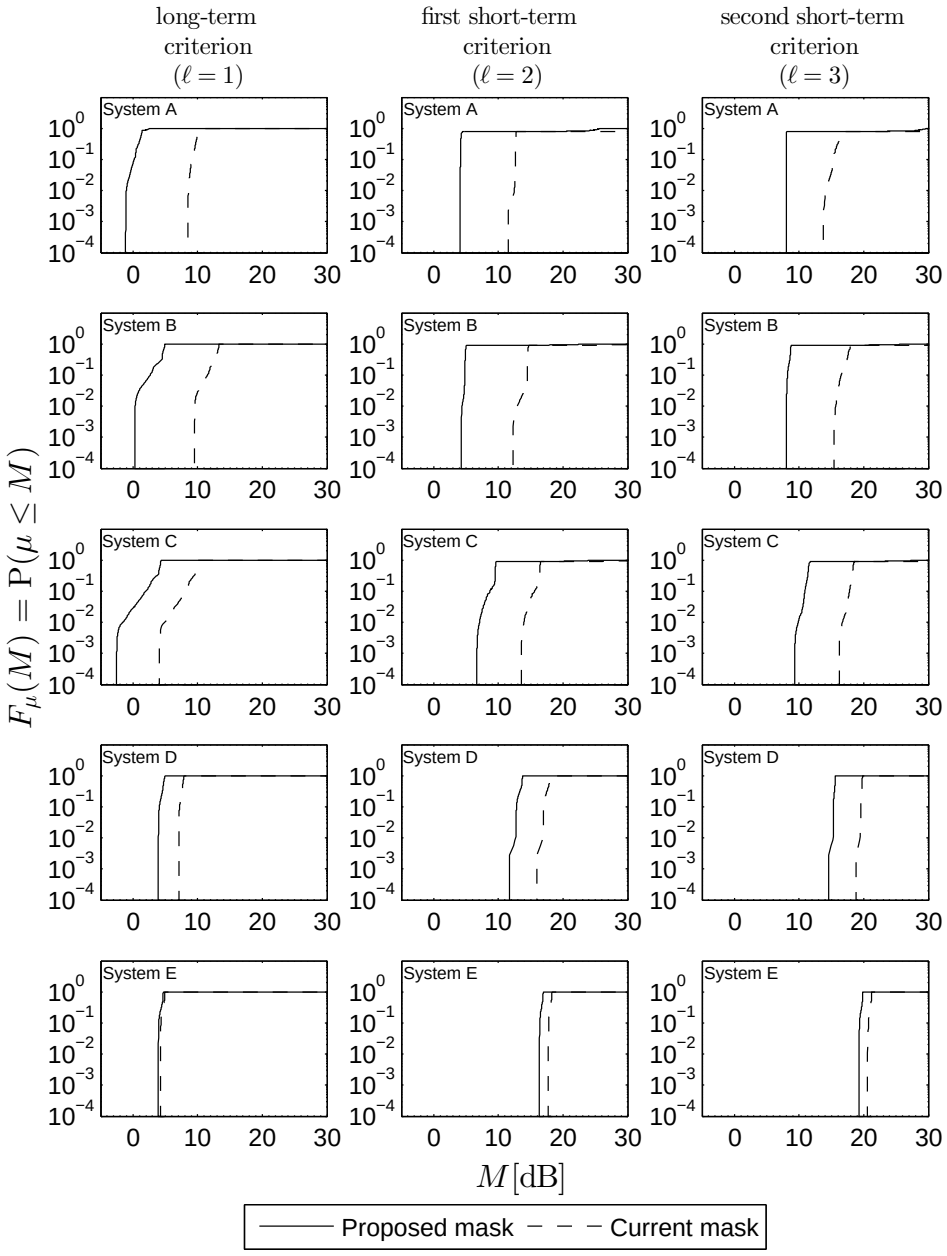

Figure 4.8: Probability distribution function of the interference margin μ_ℓ for a FS receiver located at latitude $\pm 20^\circ$ and FS antenna diameter 3.6 meters.

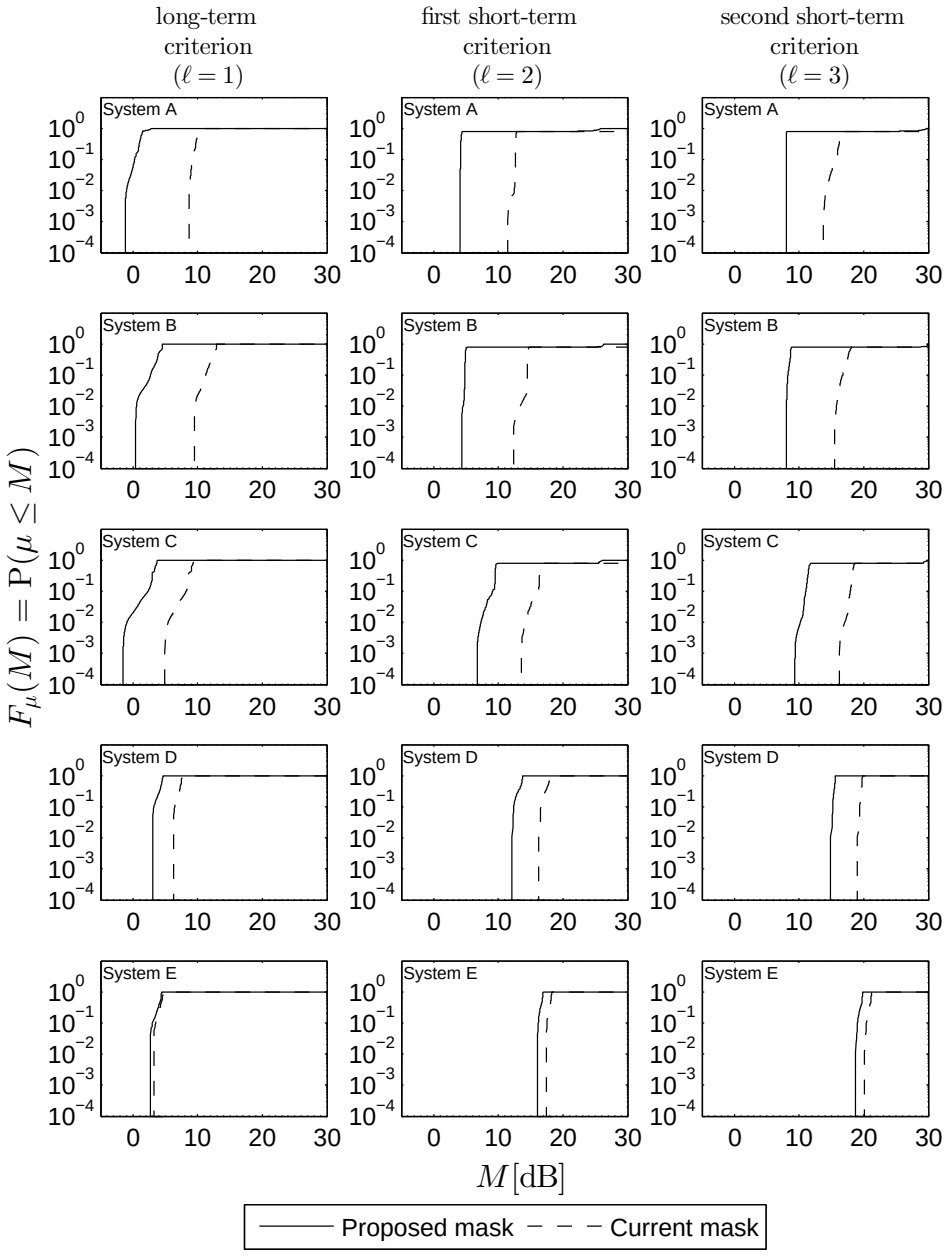

Figure 4.9: Probability distribution function of the interference margin μ_ℓ for a FS receiver located at latitude $\pm 30^\circ$ and FS antenna diameter 3.6 meters.

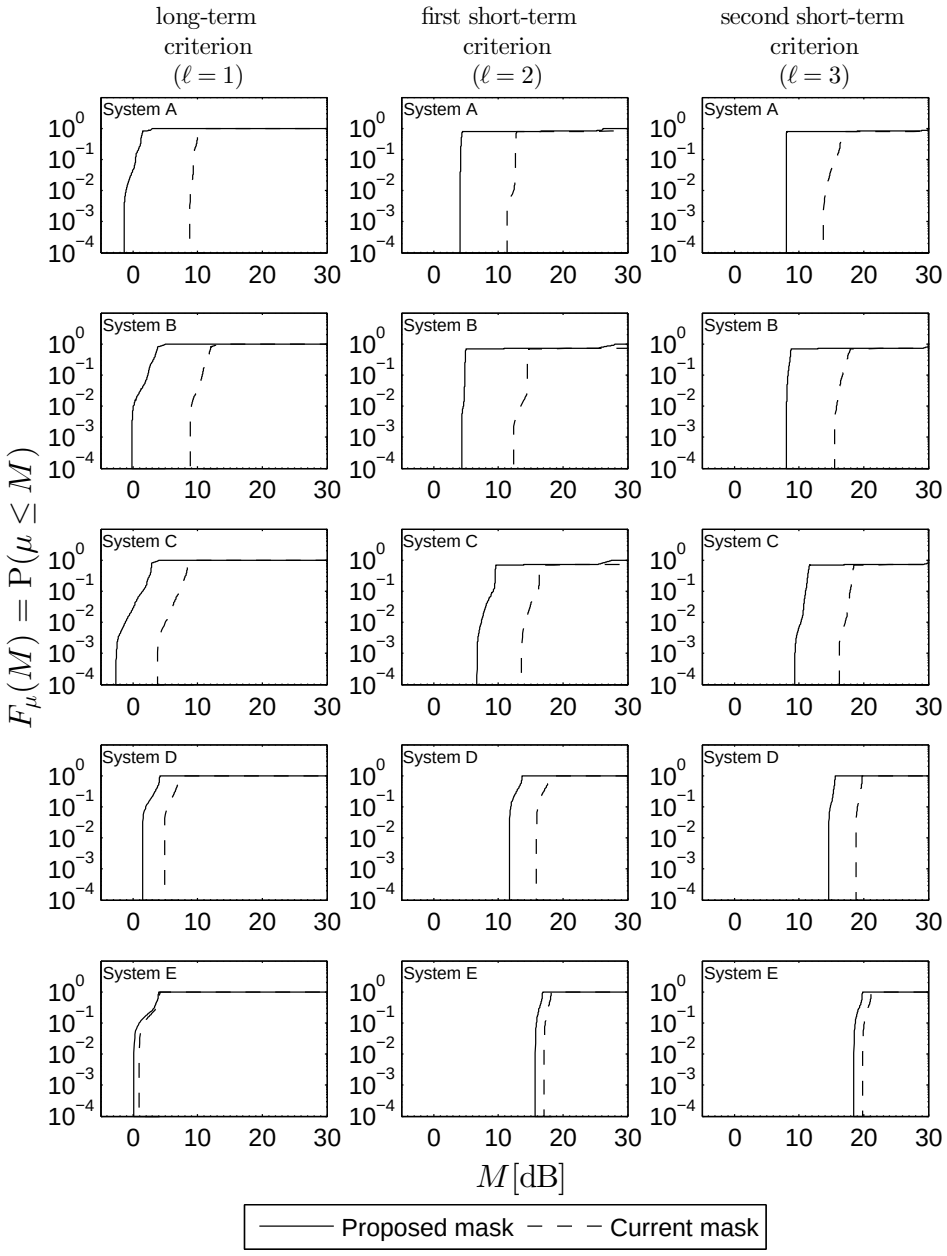

Figure 4.10: Probability distribution function of the interference margin μ_ℓ for a FS receiver located at latitude $\pm 40°$ and FS antenna diameter 3.6 meters.

The values of M_p, ΔM_p^{avg} and M_p^{min} obtained for the current and the proposed *pfd* masks are shown in tables 4.3 and 4.4 for $p = 0.999$ and $p = 0.99$, respectively.

Table 4.3: Margin Levels (dB) exceeded with probability 0.999

FS receiver antenna diameter: 3.6m													
FS latitude		0°		±10°		±20°		±30°		±40°			
pfd mask		cur.	prop.	cur.	prop.	cur.	prop.	cur.	prop.	cur.	prop.	$\Delta M_{0.999}^{avg}$	$M_{0.999}^{min}$
	ℓ=1	8.8	-1.1	8.2	-2.1	8.5	-1.1	8.6	-1.2	8.8	-1.4	10.0	-2.1
System A	2	11.4	4.1	11.0	4.1	11.5	4.1	11.4	4.1	11.3	4.1	7.3	4.1
	3	13.7	8.1	13.7	8.1	13.7	8.1	13.7	8.1	13.7	8.1	5.7	8.1
	1	13.3	4.9	12.9	4.3	9.5	0.3	9.5	0.4	8.9	-0.1	8.9	-0.1
System B	2	14.5	4.8	14.5	4.8	12.3	4.3	12.4	4.3	12.3	4.3	8.7	4.3
	3	16.8	8.4	16.4	8.2	15.4	8.1	15.5	8.1	15.5	8.1	7.7	8.1
	1	9.9	4.1	9.4	3.4	4.1	-2.5	4.9	-1.5	3.8	-2.6	6.2	-2.6
System C	2	16.3	9.5	15.6	8.7	13.6	6.7	13.6	6.7	13.6	6.7	6.9	6.7
	3	17.9	11.0	17.7	10.9	16.2	9.3	16.2	9.4	16.2	9.4	6.9	9.3
	1	7.7	4.7	7.5	4.4	7.1	3.9	6.3	3.1	4.9	1.5	3.2	1.5
System D	2	17.5	13.3	17.3	13.1	16.0	11.7	16.2	12.1	15.9	11.7	4.2	11.7
	3	19.7	15.5	19.6	15.4	18.8	14.6	19.0	14.8	18.8	14.6	4.2	14.6
	1	4.9	4.6	4.7	4.4	4.3	3.9	3.2	2.7	0.9	0.1	0.5	0.1
System E	2	18.0	16.6	17.8	16.5	17.7	16.3	17.4	16.0	17.0	15.7	1.4	15.7
	3	21.0	19.6	20.8	19.5	20.6	19.2	20.1	18.7	19.8	18.4	1.4	18.4

Table 4.4: Margin Levels (dB) exceeded with probability 0.99

FS receiver antenna diameter: 3.6m													
FS latitude		0°		±10°		±20°		±30°		±40°			
pfd mask		cur.	prop.	cur.	prop.	cur.	prop.	cur.	prop.	cur.	prop.	$\Delta M_{0.99}^{avg}$	$M_{0.99}^{min}$
	ℓ=1	8.8	-1.1	8.3	-2.0	8.6	-1.0	8.7	-1.0	9.0	-1.1	9.9	-2.0
System A	2	11.8	4.1	11.5	4.1	12.5	4.1	12.5	4.1	12.4	4.1	8.0	4.1
	3	13.9	8.1	13.9	8.1	14.3	8.1	14.2	8.1	14.2	8.1	6.0	8.1
	1	13.3	4.9	12.9	4.3	9.6	0.3	9.6	0.5	9.1	0.1	8.9	0.1
System B	2	14.5	4.8	14.5	4.8	13.0	4.4	13.4	4.5	13.5	4.6	9.1	4.4
	3	16.9	8.4	16.4	8.2	15.7	8.1	15.8	8.1	15.8	8.1	7.9	8.1
	1	9.9	4.1	9.4	3.4	4.9	-1.5	5.4	-0.9	5.0	-1.2	6.1	-1.5
System C	2	16.3	9.5	15.6	8.7	13.9	7.1	14.2	7.3	14.2	7.4	6.9	7.1
	3	18.0	11.0	17.8	10.9	16.7	9.9	17.1	10.2	17.2	10.3	6.9	9.9
	1	7.7	4.7	7.5	4.4	7.1	3.9	6.3	3.1	4.9	1.5	3.2	1.5
System D	2	17.5	13.3	17.3	13.1	16.8	12.6	16.2	12.1	15.9	11.7	4.2	11.7
	3	19.7	15.5	19.6	15.4	19.5	15.2	19.0	14.8	18.8	14.6	4.2	14.6
	1	4.9	4.6	4.7	4.4	4.3	3.9	3.2	2.7	0.9	0.1	0.5	0.1
System E	2	18.0	16.6	17.8	16.5	17.7	16.3	17.4	16.0	17.0	15.7	1.4	15.7
	3	21.0	19.6	20.8	19.5	20.6	19.2	20.1	18.7	19.8	18.4	1.4	18.4

As indicated before, due to some of the worst case conditions considered in the interference calculation, negative margins around -2.0 dB, as those shown in tables 4.3 and 4.4 for System A (latitude ±10) and System C (latitudes ±20 and ±40), are acceptable. For every other cases, the margins levels are either positive or slightly negative.

4.3
FS receiving antenna with 4.5 meters diameter

Lastly, in this section, the probability distribution functions of the $i_t/\mathcal{N}$ margins $\{\mu_\ell, \ell = 1, 2, 3\}$ were determined for the non-GSO constellations in Table 3.1. Figures 4.11 to 4.15 present, respectively, the results obtained for FS location latitudes equal to $0°, \pm 10°, \pm 20°, \pm 30°$ and $\pm 40°$. For comparison purposes, the results corresponding to the current RR Article 21 *pfd* mask are also shown in these figures.

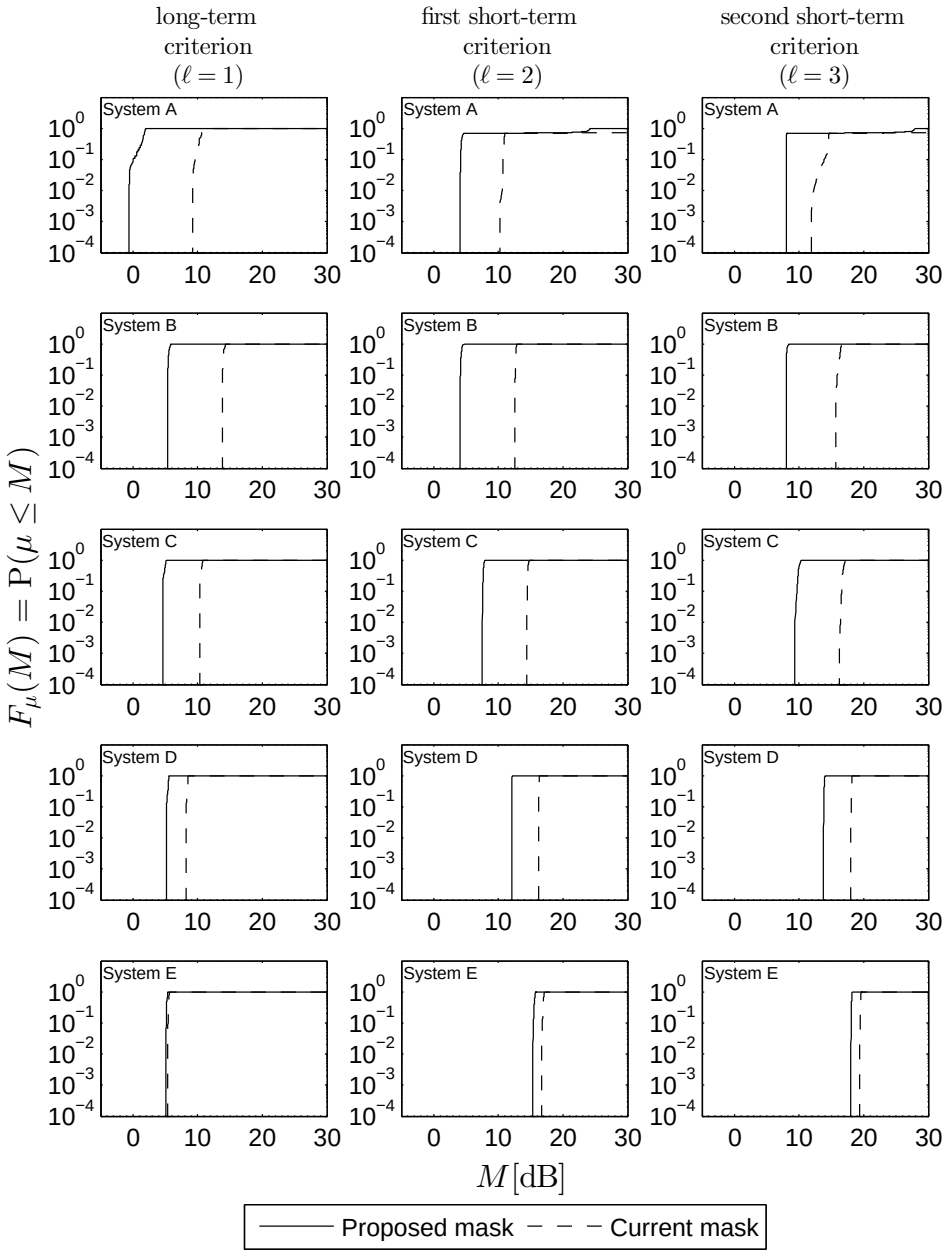

Figure 4.11: Probability distribution function of the interference margin μ_ℓ for a FS receiver located at latitude 0° and FS antenna diameter 4.5 meters.

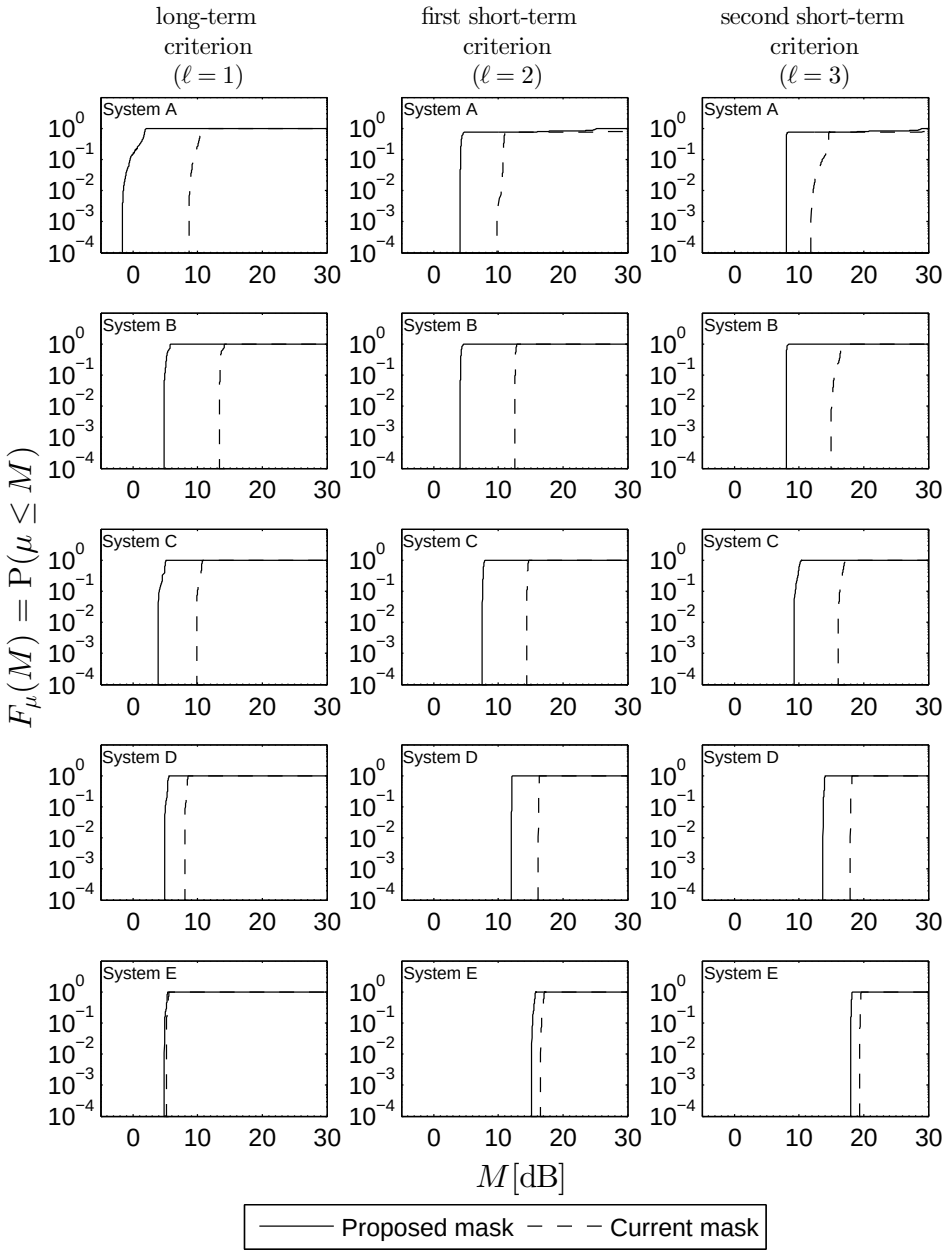

Figure 4.12: Probability distribution function of the interference margin μ_ℓ for a FS receiver located at latitude $\pm 10^\circ$ and FS antenna diameter 4.5 meters.

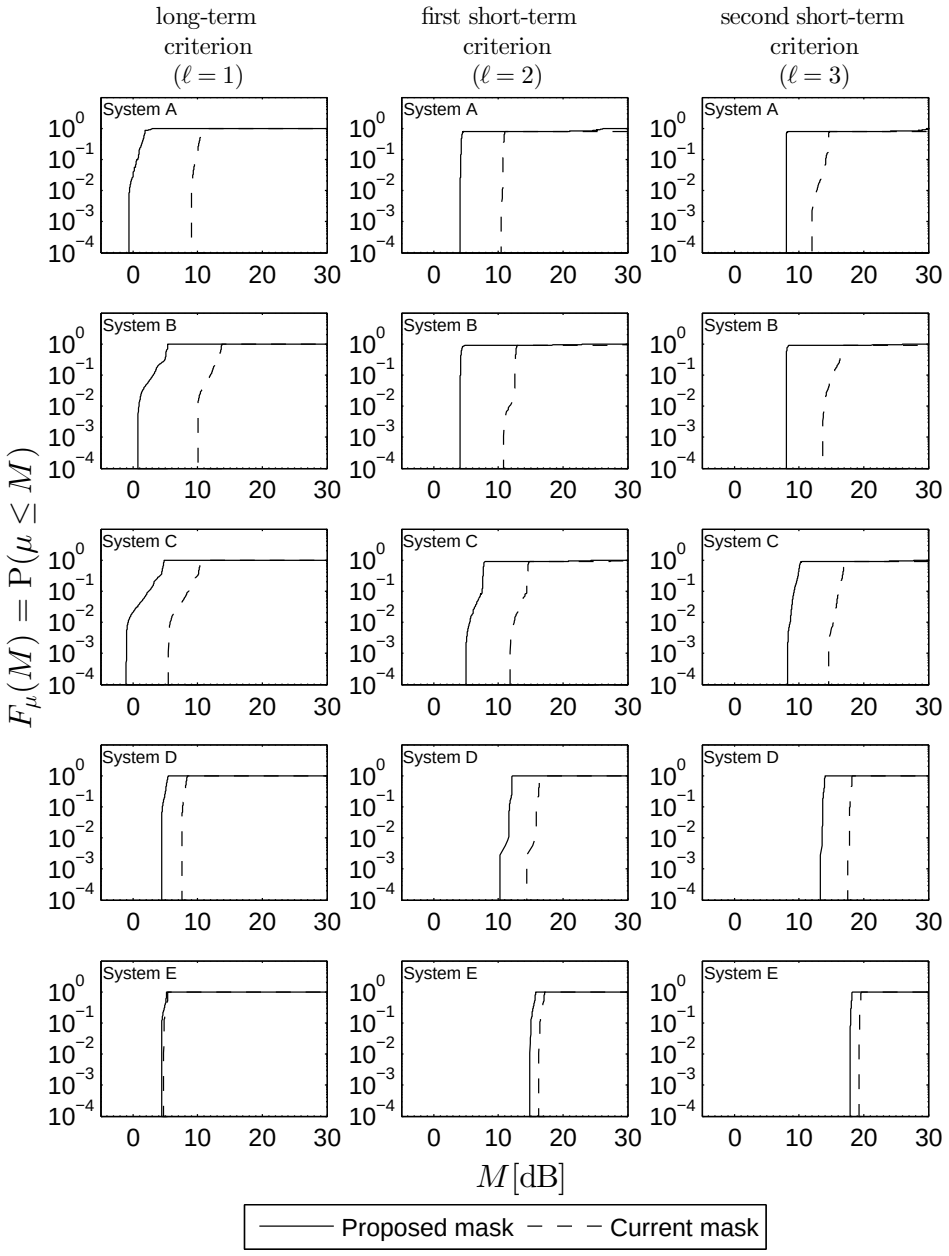

Figure 4.13: Probability distribution function of the interference margin μ_ℓ for a FS receiver located at latitude $\pm 20°$ and FS antenna diameter 4.5 meters.

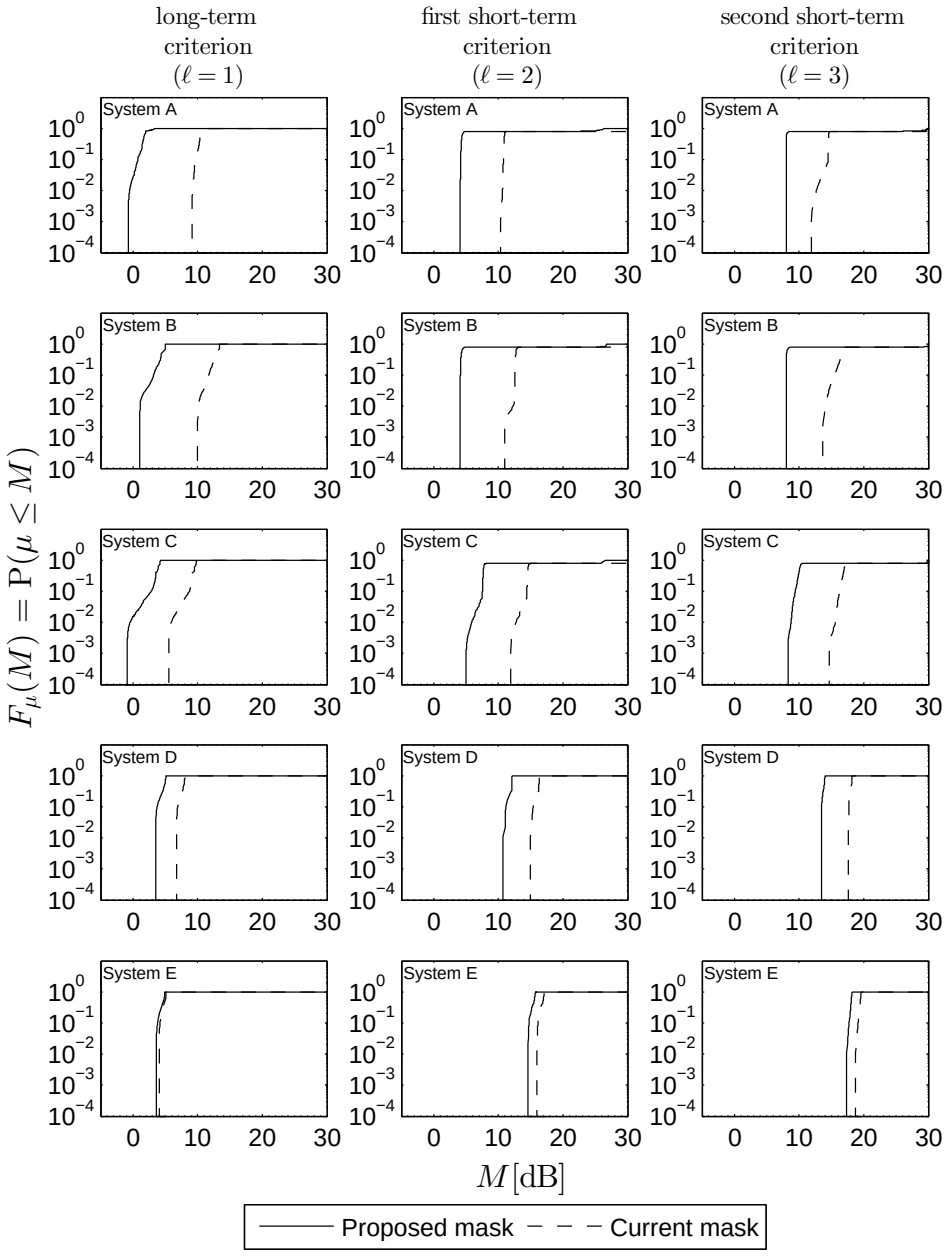

Figure 4.14: Probability distribution function of the interference margin μ_ℓ for a FS receiver located at latitude $\pm 30°$ and FS antenna diameter 4.5 meters.

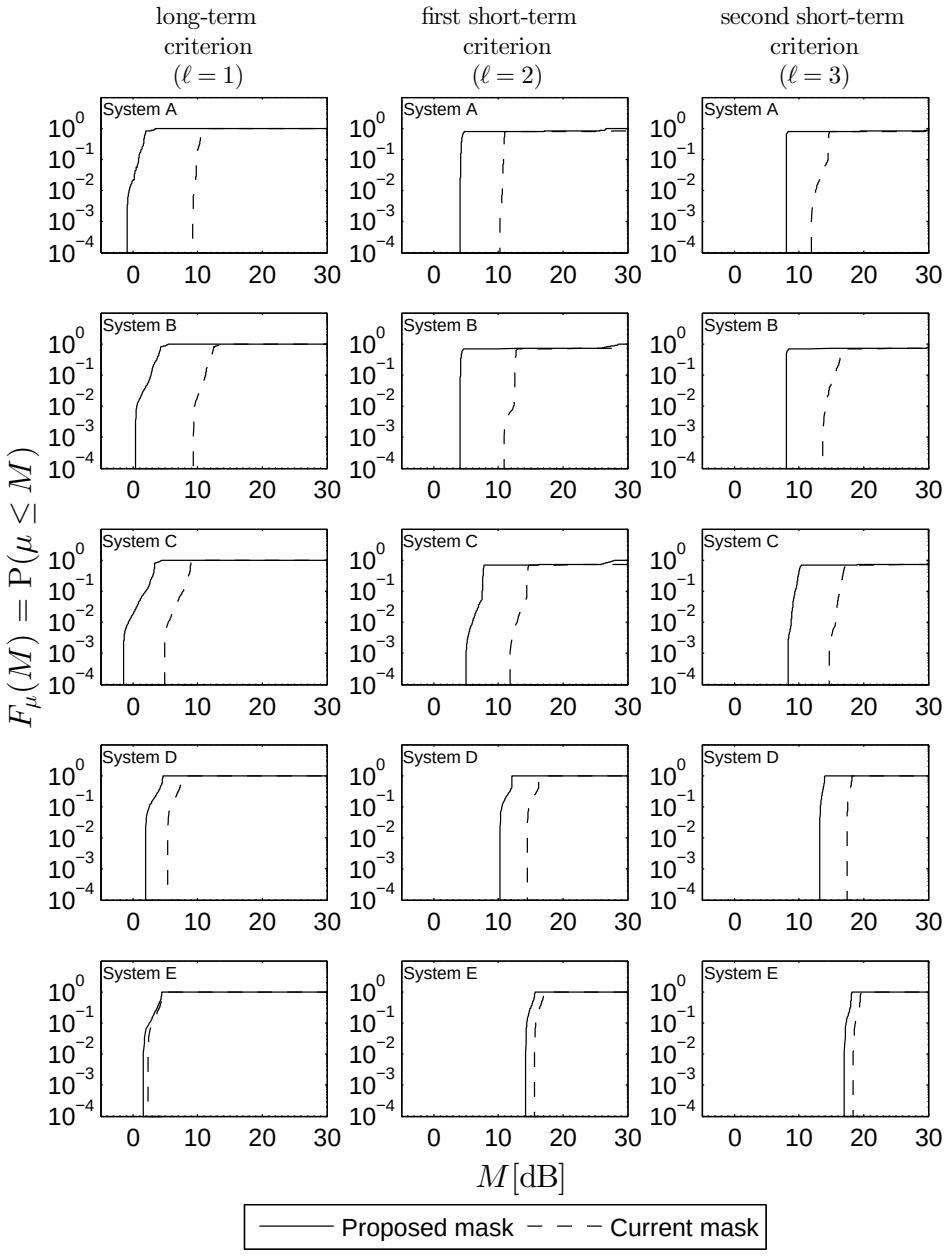

Figure 4.15: Probability distribution function of the interference margin μ_ℓ for a FS receiver located at latitude $\pm 40°$ and FS antenna diameter 4.5 meters.

The values of M_p, ΔM_p^{avg} and M_p^{min} obtained for the current and the proposed *pfd* masks are shown in tables 4.5 and 4.6 for $p = 0.999$ and $p = 0.99$, respectively.

Table 4.5: Margin Levels (dB) exceeded with probability 0.999

FS receiver antenna diameter: 4.5m													
FS latitude		0°		±10°		±20°		±30°		±40°			
pfd mask		cur.	prop.	cur.	prop.	cur.	prop.	cur.	prop.	cur.	prop.	$\Delta M_{0.999}^{avg}$	$M_{0.999}^{min}$
	ℓ=1	9.2	-0.6	8.7	-1.6	9.0	-0.6	9.1	-0.7	9.3	-0.9	10.0	-1.6
System A	2	10.2	4.1	9.8	4.1	10.4	4.1	10.4	4.1	10.2	4.1	6.1	4.1
	3	11.9	8.1	11.8	8.1	12.0	8.1	11.9	8.1	11.9	8.1	3.9	8.1
	1	13.8	5.4	13.4	4.8	10.1	0.8	10.0	1.0	9.4	0.4	8.9	0.4
System B	2	12.5	4.1	12.5	4.1	10.8	4.1	11.0	4.1	10.9	4.1	7.5	4.1
	3	15.7	8.1	15.0	8.1	13.6	8.1	13.6	8.1	13.6	8.1	6.2	8.1
	1	10.3	4.6	9.9	3.9	5.5	-1.0	5.5	-0.9	4.9	-1.5	6.2	-1.5
System C	2	14.4	7.5	14.4	7.5	11.8	5.0	11.9	5.0	11.8	5.0	6.9	5.0
	3	16.2	9.3	16.0	9.2	14.6	8.2	14.7	8.3	14.7	8.3	6.6	8.2
	1	8.2	5.2	8.0	4.9	7.6	4.4	6.8	3.5	5.4	2.0	3.2	2.0
System D	2	16.3	12.1	16.2	12.0	14.4	10.2	14.9	10.7	14.5	10.3	4.2	10.2
	3	18.0	13.8	17.9	13.7	17.5	13.3	17.6	13.4	17.4	13.2	4.2	13.2
	1	5.4	5.1	5.2	4.8	4.8	4.4	4.1	3.6	2.3	1.6	0.4	1.6
System E	2	16.6	15.3	16.5	15.1	16.3	14.9	16.0	14.6	15.6	14.2	1.4	14.2
	3	19.4	18.0	19.3	17.9	19.3	17.9	18.7	17.3	18.4	17.0	1.4	17.0

Table 4.6: Margin Levels (dB) exceeded with probability 0.99

FS receiver antenna diameter: 4.5m													
FS latitude		0°		±10°		±20°		±30°		±40°			
pfd mask		cur.	prop.	cur.	prop.	cur.	prop.	cur.	prop.	cur.	prop.	$\Delta M_{0.99}^{avg}$	$M_{0.99}^{min}$
	ℓ=1	9.2	-0.6	8.7	-1.5	9.1	-0.5	9.2	-0.5	9.4	-0.6	9.9	-1.5
System A	2	10.6	4.1	10.5	4.1	10.6	4.1	10.7	4.1	10.6	4.1	6.5	4.1
	3	12.3	8.1	12.2	8.1	12.7	8.1	12.7	8.1	12.6	8.1	4.4	8.1
	1	13.8	5.4	13.4	4.8	10.1	0.9	10.1	1.1	9.5	0.6	8.8	0.6
System B	2	12.5	4.1	12.5	4.1	11.8	4.1	12.3	4.1	12.4	4.1	8.2	4.1
	3	15.7	8.1	15.0	8.1	13.9	8.1	14.1	8.1	14.1	8.1	6.5	8.1
	1	10.3	4.6	9.9	3.9	5.7	-0.8	5.9	-0.4	5.5	-0.7	6.2	-0.8
System C	2	14.4	7.5	14.4	7.5	12.4	5.6	12.7	5.9	12.9	6.0	6.9	5.6
	3	16.4	9.3	16.1	9.2	15.3	8.6	15.6	8.7	15.7	8.8	6.9	8.6
	1	8.2	5.2	8.0	4.9	7.6	4.4	6.8	3.5	5.4	2.0	3.2	2.0
System D	2	16.3	12.1	16.2	12.0	15.7	11.5	14.9	10.7	14.5	10.3	4.2	10.3
	3	18.0	13.8	17.9	13.7	17.8	13.6	17.6	13.4	17.4	13.2	4.2	13.2
	1	5.4	5.1	5.2	4.8	4.8	4.4	4.1	3.6	2.3	1.6	0.4	1.6
System E	2	16.6	15.3	16.5	15.1	16.3	14.9	16.0	14.6	15.6	14.2	1.4	14.2
	3	19.4	18.0	19.3	17.9	19.3	17.9	18.7	17.3	18.4	17.0	1.4	17.0

As indicated in tables 4.5 and 4.6, in every case the margins levels are either positive or slightly negative.

In summary, in all considered scenarios, the proposed *pfd* limiting mask yields smaller margins than those associated with the current RR Article 21 mask, which were shown to be, in many cases, unnecessarily very high. This means that the proposed *pdfd* mask does not impose unnecessary constraints to the non-GSO satellites, as compared to the current *pfd* limits. At the same time, in all analyzed cases, the first and the second short-term criteria are met when the proposed mask is used. In most cases, the long-term criterion is met as well and, when it is not the case, it presents acceptable negative margins that occur with low probabilities. All these facts indicate that the proposed *pfd* limits are, indeed, much more adequate than the current ones.

5
Conclusion and Future Work

In this work, the current power-flux density limits in Article 21 of the Radio Regulations for non-GSO systems operating in the 3.7-4.2 GHz Band were analyzed. The analysis was motivated by Resolution 157 [1] of the World Radiocommunication Conference 2015, that recognized the need for a revision of Article 21 with a view to enabling non-GSO systems to operate in these FSS frequency bands while insuring that existing primary services (e.g. fixed service) are protected.

Initially, the mathematical and theoretical basis used to model the interference caused by multiple non-GSO satellite systems on fixed service receivers, operating in the same frequency band, was described.

In the absence of a specific protection criterion for FS systems operating in the C band, the Recommendation ITU-R F.1495 [17], which defines interference criteria to protect the Fixed Service from time-varying aggregate interference from other radiocommunication services in the 17.7-19.3 GHz band, was used to check the suitability of the current pfd limits. Aiming to analyze this current Article 21 *pfd* mask, five different circular orbit *Walker Delta type* satellite constellation structures were adequately chosen, as indicated in Table 3.1. Results have shown that the current limits impose unnecessary constraints to non-GSO systems operating in the 3.7-4.2 GHz Band.

Therefore, a methodology to investigate a more recommendable pfd limiting mask was presented. The application of this methodology led to an alternative pfd mask that approaches the pfd limits for the geostationary satellites operating in the same frequency (Table 21-4 in Article 21 of the Radio Regulations) when N=1.

The protection given to FS receivers by the proposed *pfd* mask was evaluated. Considering that the FS receiving antenna has a zero degree elevation angle and an azimuth characterized by a random variable uniformly distributed in the interval $(0°, 360°]$, the probability distribution function of the $i_t/\mathcal{N}$ margin μ_ℓ was determined for different FS receiving antenna diameters and different FS location latitudes. Due to the symmetry of the circular orbit *Walker Delta* constellation structure, the interference results do not depend on the FS location longitude. In determining these cumulative distribution

functions, the Analytical Method in [15] was used. Here, the Analytical Method was implemented using the modifications suggested in [19], for a faster and simpler computation that takes advantages of existing symmetries in the problem. For comparison purposes, the same was done with the current pfd limits.

In all analyzed scenarios, the proposed *pfd* limiting mask yielded smaller margins than those associated with the current RR Article 21 mask. This means that the proposed *pfd* mask did not impose unnecessary constraints to the non-GSO satellites, as compared to the current *pfd* limits. At the same time, in all analyzed cases, the first and the second short-term criteria were met when the proposed mask was used. In most cases, the long-term criterion was met as well. When it wasn't met, it presented acceptable negative margins that occur with low probabilities. All these facts indicated that the proposed *pfd* limits are, indeed, much more adequate than the current ones.

As indicated before, small $i_t/\mathcal{N}$ negative margins were acceptable due to some worst-case conditions considered in the interference calculations (e.g. the assumption that all satellites in the constellation produce the maximum allowed *pfd* on the Earth's surface and the use of reference antenna patterns that do not show the oscillatory behaviour present in the side-lobe gains of real antennas). Future work could consider a more realistic probabilistic model in which, for example, the *pfd* produced by the satellites on Earth's surface and the antenna side-lobe gains are modeled by random variables. It is expected that this more realistic model would mostly lead to positive $i_t/\mathcal{N}$ margins.

A
Determining the arrival and off-axis angles δ_j and γ_j

Considering Figure A.1, where the problem geometry is shown, it is straightforward to see that δ_j is complementary to the angle between the vectors $\mathbf{s}_j - \mathbf{p}$ and $\mathbf{p}$. Also that γ_j is the angle between the vectors $\mathbf{s}_j - \mathbf{p}$ and $\mathbf{a}$.

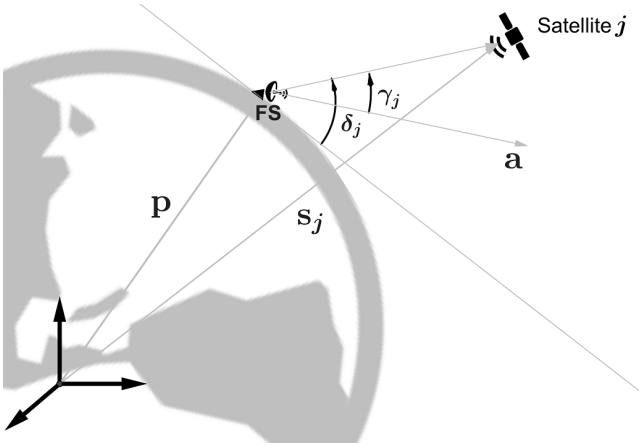

Figure A.1: Problem geometry.

The vectors $\mathbf{s}_j$ and $\mathbf{p}$ are defined in the geographic coordinate system (base B $\longrightarrow$ **ijk**), and the vector $\mathbf{a}$ is defined in a local coordinate system (base B' $\longrightarrow$ **mno**), as in Figure A.2.

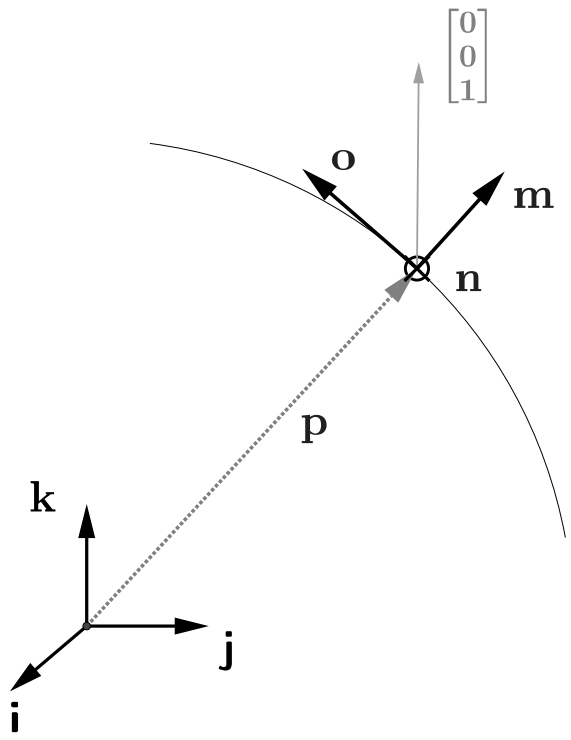

Figure A.2: Base B and base B'.

Remembering that, given two vectors in Cartesian coordinates, say $\mathbf{x}$ and $\mathbf{y}$, the angle θ between those vectors can be obtained by

$$\theta = cos^{-1}\left(\frac{\mathbf{x}^T\mathbf{y}}{\sqrt{\mathbf{x}^T\mathbf{x}\cdot\mathbf{y}^T\mathbf{y}}}\right), \tag{A-1}$$

all that is required to obtain δ_j and γ_j are the vectors $\mathbf{s}_j$, $\mathbf{p}$ and $\mathbf{a}$ in Cartesian coordinates. The vectors $\mathbf{s}_j$ and $\mathbf{p}$ are given in Spherical coordinates, a simple change of coordinates from Spherical to Cartesian can be done with the relation

$$\mathbf{x} = \begin{bmatrix} r\cos(\theta)\cos(\phi) \\ r\cos(\theta)\sin(\phi) \\ r\sin(\theta) \end{bmatrix}. \tag{A-2}$$

For the vector $\mathbf{a}$, however, since it is defined in the base B', it is necessary to perform a change of basis. The vector $\mathbf{a}$, in Cartesian coordinates on the base B', is defined by

$$\mathbf{a}_{B'} = \begin{bmatrix} \sin(\epsilon) \\ \cos(\epsilon)\sin(\alpha) \\ \cos(\epsilon)\cos(\alpha) \end{bmatrix}, \tag{A-3}$$

where the illustration of (A-3) is provided by Figure A.3.

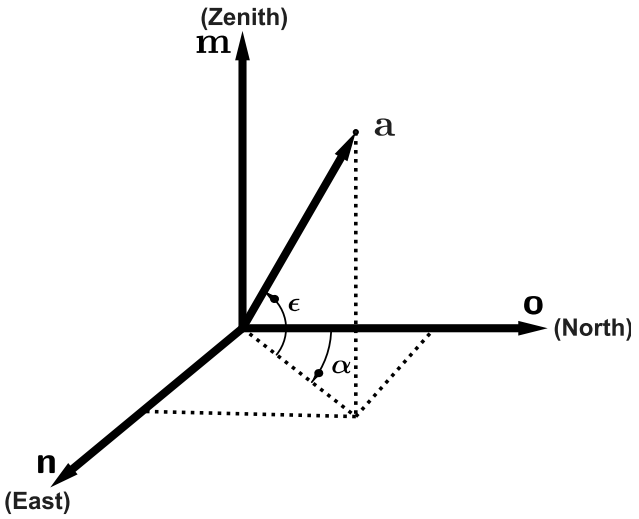

Figure A.3: Azimuth and Elevation

To represent the base B' on the base B, the relations

$$\hat{\mathbf{m}} = \frac{\mathbf{p}}{|\mathbf{p}|}, \tag{A-4}$$

also

$$\mathbf{n} = \begin{bmatrix} 0 \\ 0 \\ 1 \end{bmatrix} \times \hat{\mathbf{m}}, \tag{A-5}$$

which leads to

$$\hat{\mathbf{n}} = \frac{\mathbf{n}}{|\mathbf{n}|}, \tag{A-6}$$

and

$$\hat{\mathbf{o}} = \hat{\mathbf{m}} \times \hat{\mathbf{n}} \tag{A-7}$$

are necessary. With those relations, the matrix $\mathbf{M}$ that performs the change of basis from B' to B can be calculated. The matrix should satisfy

$$\mathbf{a}_B = \mathbf{M} \cdot \mathbf{a}_{B'}. \tag{A-8}$$

Remembering that $\mathbf{a}_{B'}$ can be written as

$$\mathbf{a}_{B'} = a_1\hat{\mathbf{m}} + a_2\hat{\mathbf{n}} + a_3\hat{\mathbf{o}}, \tag{A-9}$$

also that, from (A-4), (A-6) and (A-7),

$$\mathbf{a}_{B'} = a_1(m_1\hat{\mathbf{i}} + m_2\hat{\mathbf{j}} + m_3\hat{\mathbf{k}}) + a_2(n_1\hat{\mathbf{i}} + n_2\hat{\mathbf{j}} + n_3\hat{\mathbf{k}}) + a_3(o_1\hat{\mathbf{i}} + o_2\hat{\mathbf{j}} + o_3\hat{\mathbf{k}}), \tag{A-10}$$

which follows to

$$\mathbf{a}_B = \begin{bmatrix} m_1 & n_1 & o_1 \\ m_2 & n_2 & o_2 \\ m_3 & n_3 & o_3 \end{bmatrix} \begin{bmatrix} a_1 \\ a_2 \\ a_3 \end{bmatrix}, \tag{A-11}$$

from which can be concluded that

$$\mathbf{M} = \begin{bmatrix} m_1 & n_1 & o_1 \\ m_2 & n_2 & o_2 \\ m_3 & n_3 & o_3 \end{bmatrix}. \tag{A-12}$$

With $\mathbf{M}$, $\mathbf{a}$ can be given in the B base Cartesian coordinates. With also $\mathbf{p}$ and $\mathbf{s}$ in the B base Cartesian coordinates, δ_j and γ_j can be obtained.

Bibliography

[1] *Study of technical and operational issues and regulatory provisions for new non-geostationary-satellite orbit systems in the 3700-4200 MHz, 4500-4800 MHz, 5925-6425 MHz and 6725-7025 MHz frequency bands allocated to the fixed-satellite service*, Resolution 157, 2015 World Radiocommunication Conference Final Acts, Genebra, 2015. (document), 1, 5

[2] *Radio Regulations*, International Telecommunications Union, ITU-R, 2016. 1, 3.1

[3] *1997 World Radiocommunication Conference Final Acts*, Genebra, 1997. 1

[4] *Computer simulation of short-term interference between the feeder-links of two non-GSO MSS networks sharing the 5 and 7 GHz bands*, Document 4A/11-E, ITU-R, March 1996. 1

[5] *Interference between two NGSO FSS networks*, Document A4/101- E, ITU-R, Sep 1996. 1

[6] *Simulation of in-line interference between the feeder links of four separate non-GSO MSS constellations at 5/7 GHz (LEO-C, LEO-D, LEO-E, and LEO-F)*, Document 4A/32-E, ITU-R, Feb 1998. 1

[7] *Simulation results on the epfd calculation for NGSO FSS system operating in the 12 GHz frequency range*, Document 4A/32-E, ITU-R, Feb 1998. 1

[8] *Working document towards a preliminary draft new recommendation on frequency sharing between the non geostationary fixed satellite service (NGSO FSS) and the fixed service (FS) in the band 40.5-42.5 GHz*, Document 4A/32-E, ITU-R, Feb 1998. 1

[9] *2000 World Radiocommunication Conference Final Acts*, Istanbul, 2000. 1

[10] *Status of preliminary studies on power flux-density limits to protect the fixed service from HEO FSS satellites emissions in the 18 GHz band*, Document 4-9-S/TEMP/141-E, ITU-R, Geneva, April 2003. 1

[11] *Power Flux-density values for Satellites in the Fixed Satellite Service Using Highly Elliptical Orbits in the 4 and 11 GHz Bands*, Document 4-9-S/286-E, ITU-R, Geneva, April 2002. 1

[12] *Analysiss of Criteria for Sharing between Non-Geostationary Satellite Systems Operating in the High- Elliptical Orbits and Geostationary Networks in the Fixed Satellite Service*, Document 4A/402, ITU-R, Geneva, 2003. 1

[13] *2003 World Radiocommunication Conference Final Acts*, Geneva, 2003. 1

[14] JG Walker. *Circular Orbit Patterns Providing Continuous Whole Earth Coverage, Royal Aircraft Establishment.* Technical report, Tech. Rep. 70211 (UDC 629.195: 521.6), 1970. 2.2

[15] JMP Fortes, R Sampaio-Neto, and JE Amores Maldonado. *An analytical method for assessing interference in interference environments involving NGSO satellite networks.* International journal of satellite communications, 17(6):399–419, 1999. 2.2, 1, 4, 5

[16] José Paulo de Almeida Albuquerque, José Mauro Pedro Fortes, and Weiler Alves Finamore. *Probabilidade, variáveis aleatórias e processos estocásticos.* Editora PUC–Rio e Editora Interciência, Rio de Janeiro, Brasil, 2008. 2.3

[17] *Interference criteria to protect the fixed service from time varying aggregate interference from other radiocommunication services sharing the 17.7-19.3 GHz band on a co-primary basis*, Recommendation ITU-R F. 1495-2, 2012. 2.4, 4, 5

[18] *Mathematical model of average and related radiation patterns for line-of-sight point-to-point fixed wireless system antennas for use in certain coordination studies and interference assessment in the frequency range from 1 GHz to about 70 GHz*, Recommendation ITU-R F. 1245-2, 2012. 3.1

[19] JMP Fortes, R Sampaio-Neto, and JMO Goicochea. *Fast computation of interference statistics in multiple non-GSO satellite systems environments using the analytical method.* In *Communications, IEE Proceedings-*, volume 151, pages 44–49. IET, 2004. 4, 5